Quantifying the heat load effects of micro-hydropowered stope environments

KM Seabell

orcid.org/ 0000-0001-6671-7360

Dissertation accepted in fulfilment of the requirements for the degree *Master of Engineering in Mechanical Engineering* at the North-West University

Supervisor: Dr HJ Groenewald

Graduation: November 2023

ACKNOWLEDGEMENTS

As the author, I would like to thank everyone who assisted and supported me through the completion of this dissertation.

- Thank you to ETA Operations (Pty) Ltd and its sister companies for providing me with the opportunity and assisting me financially to complete my postgraduate studies.
- Thank you to those who provided me with guidance and academic support throughout the completion of this dissertation.
- Finally, a special thanks to those who gave me the much-needed motivation to push through and complete this dissertation.

ABSTRACT

Title: Quantifying the heat load effects of micro-hydropowered stope environments

Author: KM Seabell

Supervisor: Dr HJ Groenewald

Degree: Master of Engineering in Mechanical Engineering

Keywords: Heat load, hydropower, handheld drilling

Handheld rock drills powered by compressed air are conventionally used in underground mining operations in South Africa. Compressed air is generated using large compressors on surface, with extensive and inefficient compressed-air networks that supply underground working areas. This leads to reduced compressed-air pressure in the stopes and lower drill penetration rates. Alternative drilling technologies have been developed to combat the energy inefficiencies of compressed-air supply networks, including hydropower, electro-hydraulic and electric-powered drilling equipment. However, these new technologies add heat to the stope environment.

Additional heat can lead to increased heat injuries and reduced labourer efficiency in the workplace. Of the identified alternatives, micro-hydropower has the highest electrical heat load per drill and thus the highest probability of adding heat to the stope environment. Therefore, there is a need to quantify the heat load of micro-hydropower technologies in stope environments as the additional heat added through the introduction of micro-hydropower is largely undetermined in literature. The stope heat load was quantified through ventilation simulation modelling, which enabled the prediction of thermal changes when micro-hydropower technologies were introduced into the stope environment.

A method was developed from literature to achieve the study objectives. In this dissertation, the heat load characteristics of a stope environment were simulated to predict the thermal changes when introducing micro-hydropower technologies. The heat load was quantified by first determining the nett amount of heat added to/removed from the stope environment, determining the effect on the stope environment conditions, and analysing the effect that the conversion may have on multiple stopes in series.

A hydropowered stope conversion case study was observed and thermal-hydraulic solver simulation software was used and calibrated with empirical data captured from a real-world stope environment. The hydropowered drills were seen to add heat to the stope environment compared with a conventional stope environment equipped with compressed-air drills. The first stope's reject wet-bulb temperature increased by 0.6 °C. Thereafter, the simulation was extended to predict the thermal changes along a micro-hydropower converted raise line. By the third stope environment, the wet-bulb temperature of the micro-hydropowered environment was 1.8 °C hotter than the compressed-air raise line environment. This implies that the hydropower raise line will be at a greater risk of heat injuries and will experience a reduction of labourer efficiency because of the higher temperatures.

TABLE OF CONTENTS

LIST OF FIGURES

LIST OF TABLES

NOMENCLATURE

Symbol	Description	Units
A	Area	m²
bar	Unit of pressure	100 kPa
C_p	Specific heat capacity	kJ/kg°C
H	Height	m
h	Enthalpy	J/kg
	Frequency	Hz
	Pressure	kPa
L	length	m
$\dot{m}$	Mass flow	kg/s
P	Power	kW
Q	Heat	kW
RoP	Rate of penetration	m/min
T	Temperature	°C
$\boldsymbol{V}$	Voltage	V
$\boldsymbol{W}$	Width	m

LIST OF ABBREVIATIONS

3D	Three-dimensional
CFD	Computational Fluid Dynamics
DXF	Drawing eXchange Format
KPI	Key Performance Indicator
LOM	Life of Mine
MAE	Mean Absolute Error
UG2	Upper Group 2 Chromitite Reef

CHAPTER 1 – INTRODUCTION AND LITERATURE

1.1 Preamble

The first chapter introduces the conventional underground mining practices in South Africa and the challenges faced with the use of pneumatic handheld rock drills. The chapter explores the alternative drilling technologies that aim to combat the inefficiencies of conventional drilling. From this analysis, a literature study is done to identify a gap in the knowledge base of alternative drilling technologies in underground mines. A problem statement for this dissertation is formulated with objectives for the study to fulfil the identified knowledge gap.

1.2 Conventional underground mining practice

The South African Bushveld Complex is the world's largest layered tabular intrusion of mineral deposits and is famous for its platinum-group element deposits [1]–[3]. In this region, there is a near constant width (40–120 cm) and near constant grade (5–8 g/t) reef ranging over more than 100 km, called the Merensky Reef [2]. Another main economic deposit in the Bushveld Complex is the Upper Group 2 (UG2) chromitite reef, which is found about 20 m beneath the Merensky Reef in some regions [1].

The conventional mining method in underground South African mines is narrow tabular orebody mining [4]. Although it generally results in the least ore and waste dilution, the method is labour-intensive [4], [5].

Narrow tabular orebody mining is favoured in the South African gold and platinum mining industry due to the typical width of the reef/orebody being less than 1 m [6]. The reef in the Bushveld Complex is characterised by a continuous downward dipping and steplike formation of the stratigraphy [3]. This formation and characterisation of the Bushveld Complex are illustrated in Figure 1-1. The various reef layers are seen to angle/incline downwards from left to right in the depiction, with a steep stepdown in the middle of the region.

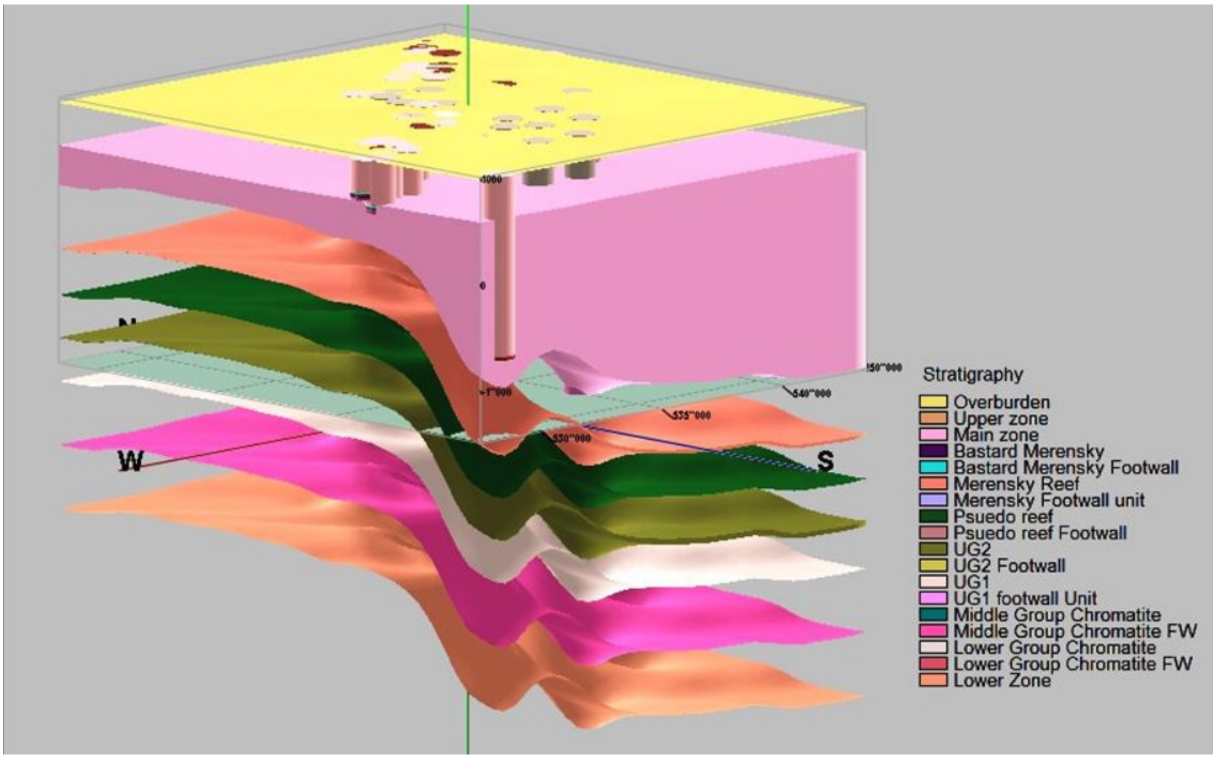

Figure 1-1: Bushveld Complex stratigraphy [3]

The angle at which the reef inclines horizontally in the rock structure is referred to as the dip angle [7]. Typical dip angles in South African gold and platinum mines range between 0° and 30°, and average between 8° and 14° [8], [9]. There are also discontinuities in the reef due to the presence of different geological structures. Examples of these geographical discontinuities are rolling reef, potholes, faults and dykes [4]. In rolling reef, the reef may roll in sections with a wavelength between 2 m and 12 m and have a vertical separation of up to 6 m [10]. Figure 1-2 illustrates the rolling reef discontinuity that is expected to be seen in the step region of Figure 1-1. Figure 1-2 shows that the dip angle of the reef changes rapidly in the rolling reef discontinuity.

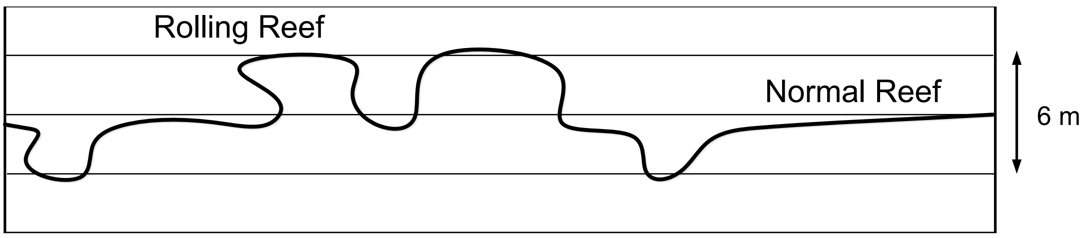

Figure 1-2: Merensky reef variations[1]

[1] Adapted from [61].

Mechanised mining methods, referred to as trackless mining, have been introduced to South Africa and are predominantly used in coal and copper mining operations where the stoping width is more than 1.8 m [6]. However, due to the generally narrow-reef orebodies in the gold and platinum industry, the already developed mechanised equipment used in the coal and copper mines needs to be adapted and re-engineered to suit the narrow tabular orebody mining environment [6]. However, mechanised mining equipment is limited in its capabilities when dip angles exceed their design angle, typically 10–16° [7], [8]. Greater dip angles increase the loading on breaking components of mechanised equipment, and traction limitations become prevalent when the dip angle is more than 20° [9], [11].

A high frequency of geological discontinuities in the orebody is unfavourable in mechanised mining methods as discontinuities affect the grade of the ore mined through dilution and reduce production due to machine interruptions [7]. The dilution is caused by mining waste material above or below the reef seam and machine interruptions because of the repositioning the mechanised equipment. According to Moxham [6], because of ore dilution and orebody constraints, most gold and platinum mines where trackless mining was introduced have returned to using handheld rock drills. This type of mining is referred to as the conventional mining method in this dissertation.

1.3 Conventional pneumatic handheld rock drill

Handheld rock drills in South African mines, such as replicas of the S215 or S25 pneumatic rock drills by Boart Longyear, are conventionally/predominantly powered by compressed air [12], [13]. These pneumatic rock drills have been an industry standard in South Africa since the 1970s [14]. The latest iteration of the pneumatic rock drills from Boart Longyear is the S250. However, Boart Longyear discontinued this range, with the end-of-life date set for December 2022.[2] Figure 1-3 illustrates a typical pneumatic rock drill set-up.

[2] Boart Longyear. (n.d.). *Notification of discontinuance: S250 Rock Drill*. Retrieved June 4, 2022, from https://www.boartlongyear.com/product/s250-rock-drill/

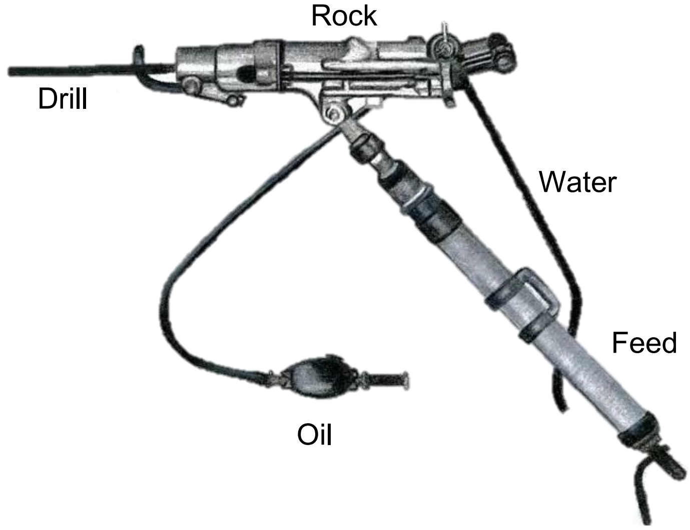

Figure 1-3: Typical pneumatic rock drill set-up[3]

As seen in Figure 1-3, the compressed air supplied by the mine is supplied through an air hose. An oiler is connected before the rock drill on the air hose to provide lubrication to the drill. Pneumatic rock drills use compressed air for the percussion and rotation of the drill steel and for the thrust of the drill into the rockface from the air/feed leg [15]. A water hose supplies the water required for flushing the drill bit and drilled hole. A typical pneumatic stope layout is depicted in Figure 1-4.

Figure 1-4 shows that the mine supply water and compressed air are routed to a manifold near the active panel. Thereafter, compressed-air and water hoses are connected to the manifolds and supply each pneumatic drill individually. Two types of drills are used in the stope environment, namely a rockface drill and a roof bolter drill. A rockface drill is used to drill a hole into the orebody face and advanced strike gully of the panel. Advanced strike gullies provide access to the orebody face and enable the removal of ore from the face. After drilling, explosives are inserted into the drilled holes [16].

Centre gullies enable the removal of ore from multiple advanced strike gullies. These drills provide horizontal development into the orebody of the stope. A roof bolting/bolter drill is used to drill vertical holes into the roof of the panel. These holes are later loaded with roof bolts that provide support to the stope roof by making the roof self-supporting.[4]

[3] Bisbee Mining & Minerals. (n.d.). Jackleg. Retrieved July 5, 2023, from https://www.bisbeeminingandminerals.com/jackleg

[4] Anglo American. (n.d.). *Mining terms explained: A to Z*. Retrieved July 4, 2023, from https://www.angloamerican.com/futuresmart/stories/our-world/environment/mining-terms-explained-a-to-z

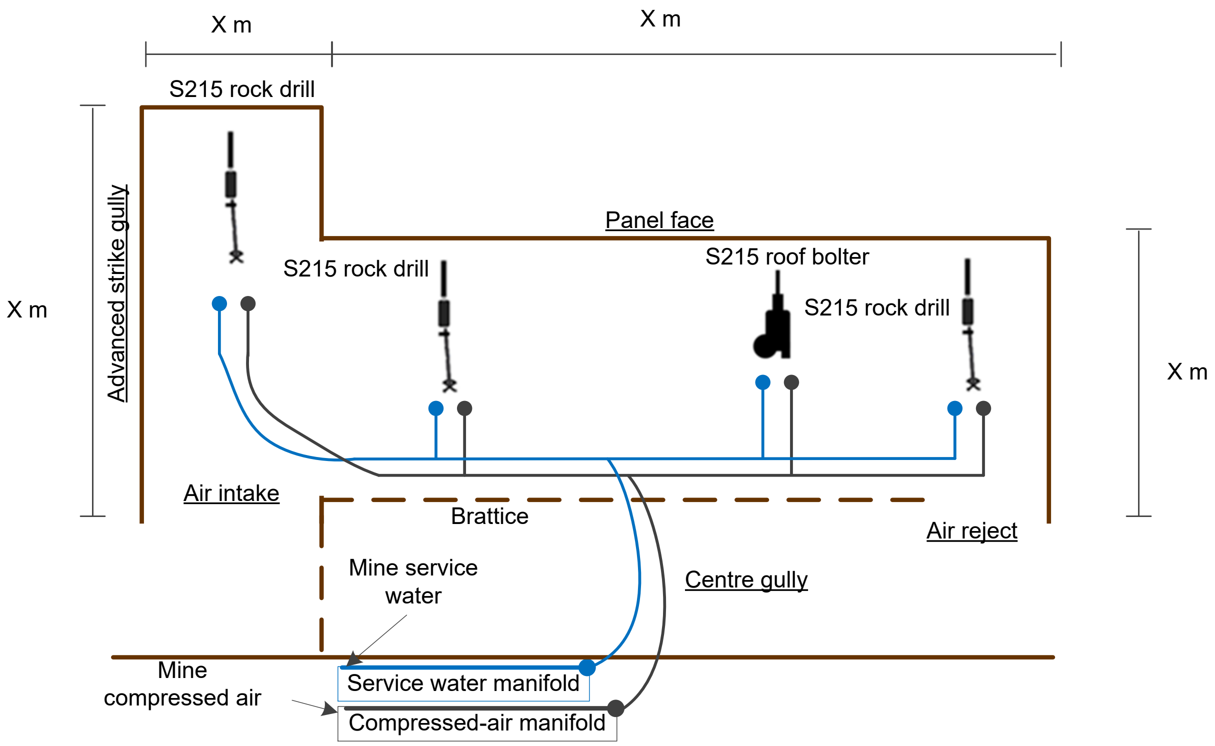

Figure 1-4: Typical pneumatic stope layout[5]

Compressed air is expanded at the outlet port of the drill through the operation of pneumatic drills. The rapid expansion of the gas decreases its temperature due to adiabatic expansion [17]. This reduces the temperature in the localised area around the drill. The temperature reduction phenomenon can be observed on the drills themselves through ice formation. An example of this phenomenon is shown in Figure 1-5.

Figure 1-5: Ice formation on compressed-air drill.[6]

[5] Illustration by author.

[6] Photo taken by B. van Rooyen on a gold mine in South Africa.

1.3.1 Compressed-air inefficiencies and penetration rate

The use of pneumatic rock drills is largely energy inefficient. Of the energy used to generate the compressed air on surface, only 2–4% is available at the face/stope for drilling operations [12], [18]. The large inefficiency is not because of the pneumatic equipment itself, but rather the large compressed-air network needed to supply the pneumatic equipment [19]. The size of compressed-air networks is extensive when considering the total surface piping network. Some underground mines in South Africa are over four kilometres deep [20]. The distance from the station to the active working areas in ageing mines can exceed four kilometres. According to Marais [20], underground piping networks could be up to eight kilometres in length away from the surface compressed-air network. This is a result of the long travelling distances to active working areas and the depth of the mine itself.

The efficiency of the overall system decreases over time as mining operations mature and grow in size and complexity. Efficiency loss is due to increasing line losses, leaks and misuse of the resource for ventilation of the local environment [19]. These losses reduce the pressures in the compressed-air supply for the rock drills [21]. The penetration rate of the rock drills is thus reduced as the penetration rate and compressed-air supply pressure are directly related.

Figure 1-6 shows that with a reduction in pressure from 550 kPa to 450 kPa, the penetration rate of a standard S215 rock drill reduces by 0.2 m/min, thus reducing the productivity of the drills.

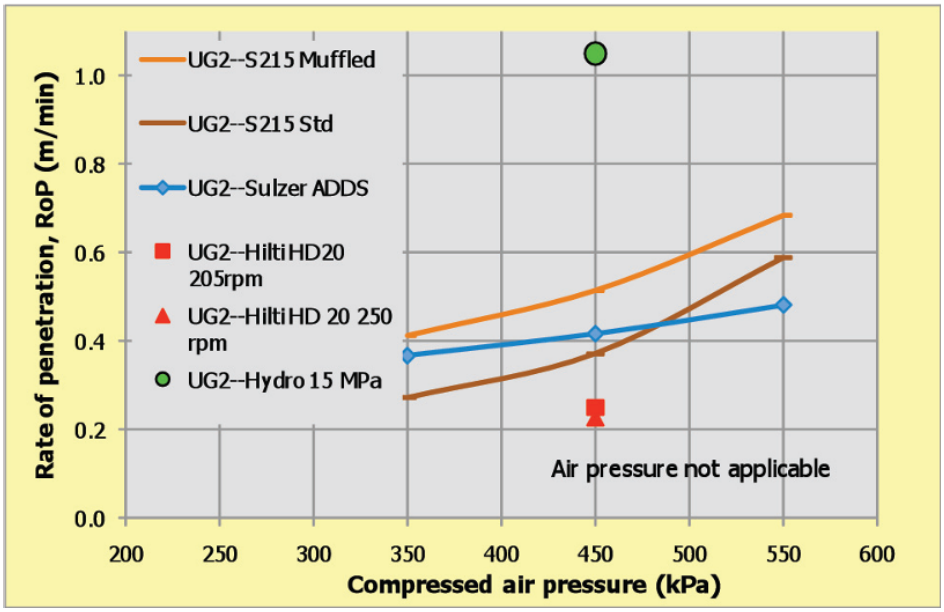

Figure 1-6: Drill rates of penetration in UG2 [22]

1.3.2 Health and safety concerns

Pneumatic drills are generally lubricated by grease/air oil that is inserted into the compressed-air supply through an inline air lubricator or oiler [23]. The oiler needed to lubricate the mechanical components of the drill is shown in Figure 1-3. However, the oil is expelled into the environment through the exhaust of the pneumatic drill, which exposes the rock drill operator and surrounding crew to atomised oil particles [23].[7] These oil particles create a fogging or misting of the stope environment [24]. Aspirated rock drill oil may cause chemical pneumonia [25]. A study done by Nowak [26] investigated the health effects of lubricated oils emitted into the environment for systems with open cutting systems, such as saws and harvesters. The oil mist generated through operation gets into the respiratory tract and causes changes to not only the lungs but also the kidneys, heart, liver and adrenal glands. Additionally, people in long-term contact with oil mist show a higher prevalence of cancer, most often skin cancer.

1.3.3 The need for alternative drilling technologies

From the investigation into conventional underground mining practices and handheld drills, it is clear that there are inherent problems with extensive underground compressed-air networks. These problems are negatively affecting the performance of compressed-air rock drills.

Compressed-air rock drills further introduce health and safety concerns into the stope environment through atomised oil particles. Thus, there exists a need for an alternative drilling technology that addresses the issue of the reducing penetration rates of pneumatic rock drills and their associated health and safety concerns.

1.4 Advancements in drilling alternatives

There are several manufacturers of alternative drilling solutions, which are classified by their main operating philosophy. These include electro-hydraulic, electric and hydropower alternative drilling technologies. These technologies all claim benefits and advantages over pneumatic drills such as increased penetration rates, lower noise levels, lower energy consumption, reduced operator fatigue, improved water consumption and increased production, to name a few [12], [18], [19]. The above-mentioned alternate drilling technologies are elaborated in Sections 1.4.1–1.4.3.

[7] Michaud, D. (2017, February 9). Electric rock drill. *911 Metallurgist*. Retrieved from https://www.911metallurgist.com/electric-rock-drill/

1.4.1 Electro-hydraulic technology

Hydraulic or electro-hydraulic handheld rock drills use highly pressurised hydraulic fluid to power the handheld drills. The hydraulic fluid is pressurised by the power pack, which is the power transmitter of the system [27]. Epiroc is a Swedish manufacturer of industrial equipment that has been manufacturing a wide range of pneumatic handheld rockdrills dating back to the 1930s, when they introduced their first lightweight pneumatic handheld rock drill. However, their latest handheld rock drill, namely the RD100/HRD100, is an electro-hydraulic alternative [23].[8] In electro-hydraulic handheld rock drills such as the RD100, the hydraulic fluid is pressurised to 120 bar from its 10 kW PP100 power pack [28].

The power pack needs to be situated close to the drill and thus has to be in the stope environment. Additionally, for a stoping crew operating four drills, four power packs are needed, thereby summating to an additional 40 kW of electrical heat load in the stope. According to Epiroc [28], the drill rate of the RD100 is 200% faster than a pneumatic drill at 5 bar air pressure, and the energy consumption is reduced by 450%. Figure 1-7 shows the electro-hydraulic RD100 rock drill and PP100 power pack to illustrate the in-stope system set-up required for one rock drill operator.

Figure 1-7: Epiroc RD100 and PP100[9]

[8] Epiroc. (n.d.). Handheld drilling tools. Retrieved July 5, 2023, from https://www.epiroc.com/en-za/products/rock-drilling-tools/handheld-drilling-tools
[9] Epiroc. (n.d.). HRD100: Hydraulic rock drill. Retrieved July 5, 2023, from https://www.epiroc.com/en-ge/products/rock-drilling-tools/handheld-drilling-tools

For the Epiroc system to be operational in the stope environment, a water supply of between 5 bar and 8 bar of pressure is needed for cooling the power pack, flushing the drill bit and thrusting the pusher leg. The 10 kW power pack requires a 440–525 V, 50 Hz electrical supply [28]. The typical stope layout for an electro-hydraulic system is depicted in Figure 1-8.

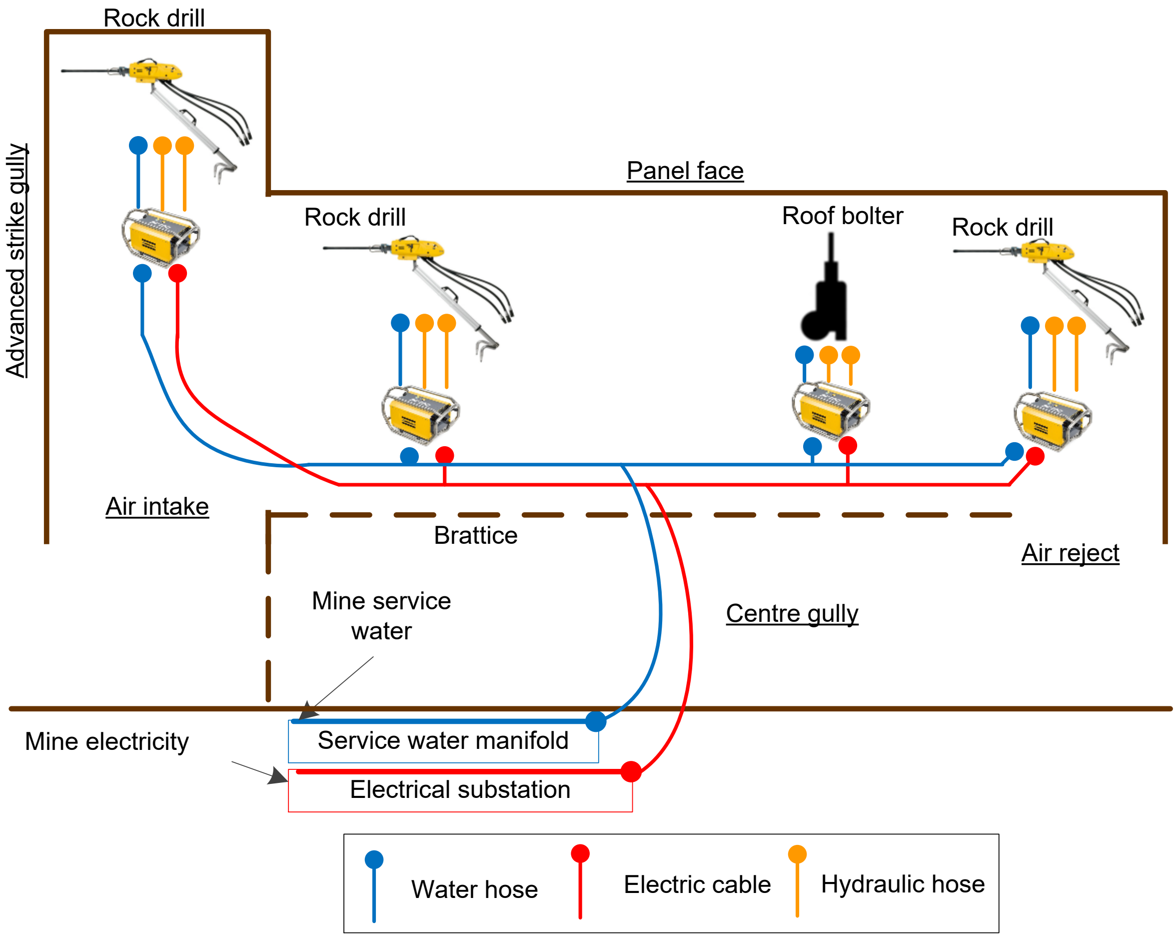

Figure 1-8: Typical electro-hydraulic stope layout[10]

Similar to the pneumatic stope layout of Figure 1-4, the electro-hydraulic stope layout in Figure 1-8 requires the same water reticulation layout. However, an electrical substation is needed near the stope to supply the individual power packs through electrical cables. From each power pack, two hydraulic hoses (supply and return) and one water hose supply each drill. The individual drill set-up can be seen in Figure 1-7.

Other benefits stated by Epiroc and users of the drills include 50% lower noise emission, improved water control, lower vibrations and improved air quality [28], [29]. The water-on-demand system

[10] Illustration by author.

that the HRD100 incorporates is an automatic water control system. This system switches the flushing water of the drill off when not in use, thus reducing water consumption [28]. The air quality around the rock drill operator is also improved by eliminating the atomised oil into the environment [29]. David Baird, the global product manager of Epiroc, states that the HRD100 meets the requirements of South Africa's increasing electricity supply restraints and that the demand for hydraulic tools is expected to increase significantly.[11]

1.4.2 Electric technology

Hilti electric handheld rock drills originated from the request of a South African gold mine. AngloGold Ashanti were investigating alternate energy sources for rock drilling in 1996 [18]. They requested Hilti to investigate the feasibility of electrically powered handheld rock drills in their stopes and development ends. Both parties agreed on the possible success of the investigation. This led to the development and implementation of electric handheld rock drills in AngloGold's Tau Tona Gold mine in South Africa.

The 2.2 kW Hilti TE MD20 electric handheld rock drill requires a 240 V, 50–60 Hz electrical supply in the stope. For a crew of four, there is thus an additional electrical heat load of 8.8 kW per stope. The drill needs to be supplied with water at a minimum of 3 bar water pressure [30]. The water is used in the pusher leg to provide thrust, to cool the drill, and to flush and cool the drill bit. A typical stope layout for electric rock drills is depicted in Figure 1-9.

The stope layout for electric rock drills is the same as that of the electro-hydraulic drills in Figure 1-8. However, the water hose and electrical supply cables are connected directly to the drills themselves. Electrically powered handheld rock drills have a range of advantages over conventional pneumatic drills. According to Van Jaarsveld [18], these advantages include:

- Quieter and less vibration.
- More energy efficient.
- Can be used in areas of poor compressed-air reticulation.
- Improved environment visibility: no fogging and misting as seen in pneumatic stopes.
- Reduced operator drill times.
- Possibility of in-stope lighting.

[11] Engineering News. (2022, May 24). Efficient, fast, accurate, clean and safe drilling with Epiroc HRD100 Hydraulic Rock Drill. https://www.engineeringnews.co.za/print-version/efficient-fast-accurate-clean-and-safe-drilling-with-epiroc-hrd100-hydraulic-rock-drill-2022-05-24

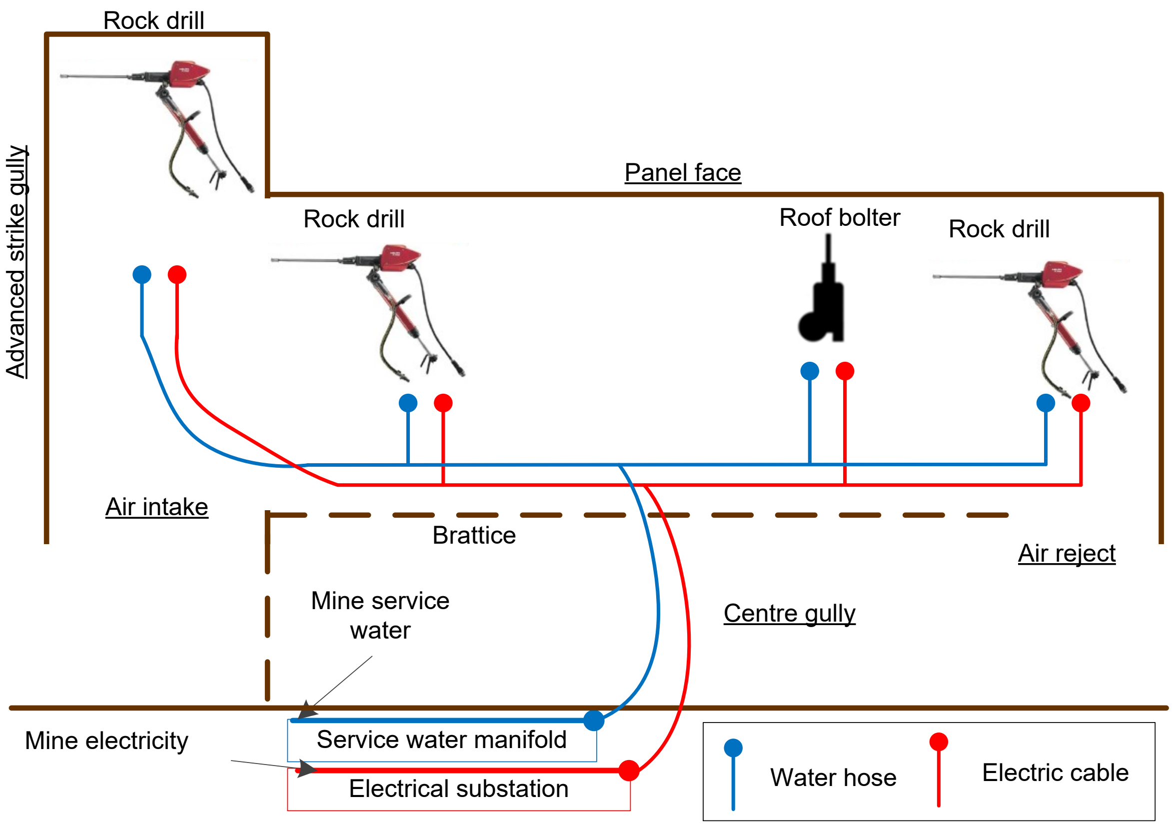

Figure 1-9: Typical electric rock drill stope layout[12]

Some of these advantages hinge on the inherent inefficiency of compressed-air systems as discussed previously. However, the possibility of in-stope lighting is a unique advantage of electrifying the stope environment. Similar to electro-hydraulic systems, the electric handheld rock drill does not impair the air quality around the operators as there is no atomised lubricating oil as discussed in Section 1.3.2 regarding pneumatic rock drills.

The penetration rates for various handheld rockdrills technologies were compared in a study done by Fraser [22]. Two rock types were used in the comparison, namely norite and UG2. Norite is a rock type that is layered in the Merensky Reef, and UG2 is a chromitite rock type rich in platinum-group elements [31].

From Table 1-1 it is clear that the penetration rate of the Hilti TE MD 20 is significantly lower than that of the hydropower and pneumatic alternatives. The Hilti TE MD 20 had been developed over 12 years in collaboration with AngloGold Ashanti. Their vison was creating a better working environment and combating the reducing penetration rates of their conventional drills [18], [32].

[12] Illustration by author.

Table 1-1: Drill penetration rates [22]

Drill performance Rock type	Type	Pressure [MPa]	Rate of penetration [m/min]	
			Norite	UG2
Sulzer-New gen hydro	Hydro	15.00	0.70	1.05
Boart Longyear-S215 muffled	Pneumatic	0.45	0.25	0.56
Boart Longyear-S215 standard	Pneumatic	0.45	0.28	0.40
Sulzer-ADDS water-lubricated	Pneumatic	0.45	0.28	0.46
Industry average drill in quartzite	Pneumatic	0.45	0.19	0.30
Hilti TE MD 20 electric	Electric	n/a	0.13	0.30

An electric drill was chosen due to its ability to perform at the same rate regardless of its location. In 2007, the Hilti TE rock drill was rolled out on AngloGold's Tau Tona Gold mine in South Africa [18]. The Hilti rock drill achieved an average penetration rate of 0.29 m/min, which was an improvement on their existing compressed-air rock drills. However, the poor performance of the compressed-air rock drills was due to the mine's insufficient compressed-air reticulation network [18].

Comparisons between an adequately supplied compressed-air rock drill were done at 430 kPa compressed-air pressure, and the compressed-air rock drill had a penetration rate of 0.39 m/min. Therefore, the success on Tau Tona was largely due to their poor compressed-air reticulation network.

1.4.3 Hydropower technology

The last of the alternative drilling solutions to be discussed is hydropower technology. There are three main types of hydropower systems, micro, localised and centralised. Centralised systems are generally gravity-fed from the main shaft column with mining depths in excess of 1.8 km. This mining depth is necessary for there to be enough potential energy in the water column as 18 MPa of water pressure is generally required for hydropower applications [33]. A centralised hydropower column is shown in Figure 1-10 supplying multiple levels with a high-pressure water supply line.

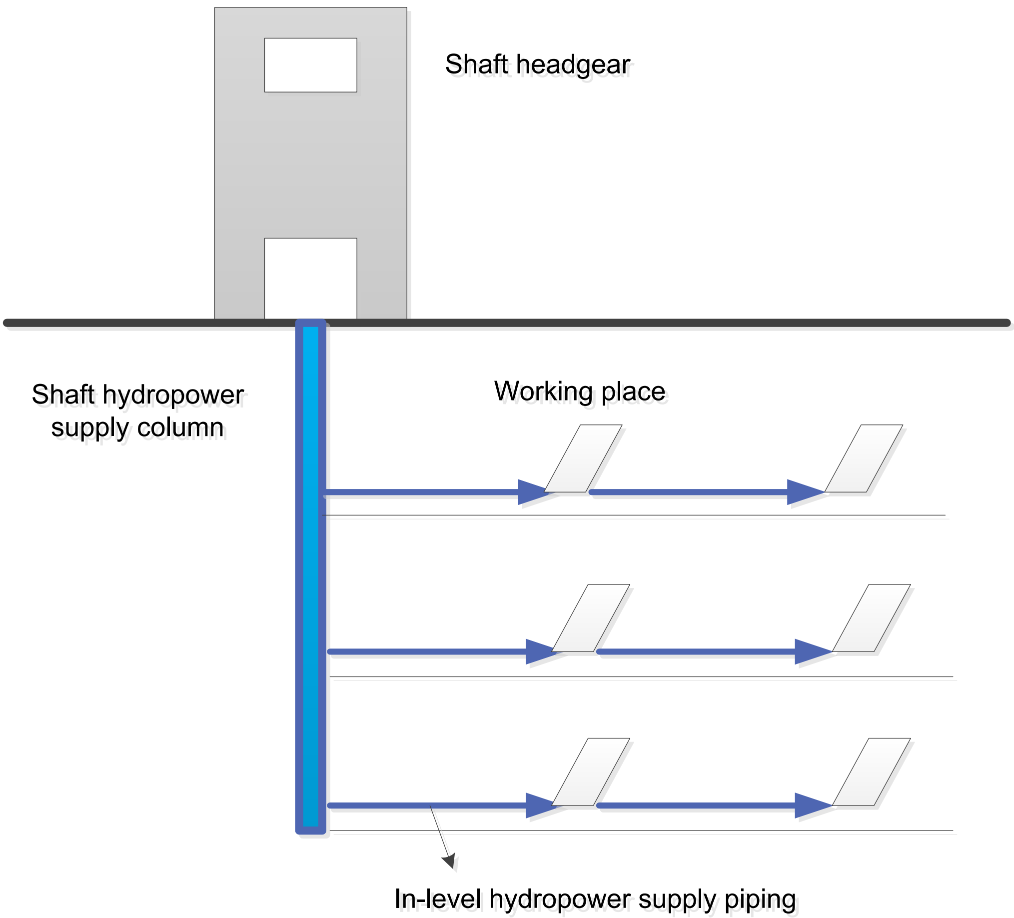

Figure 1-10: Centralised hydropower network[13]

The water reticulation network for centralised hydropower is similar to a regular service water reticulation network; however, because the network operates at higher pressures, higher pressure rated pipes are needed. Centralised systems require larger capital investment and maintenance costs than localised and micro-hydropower systems as larger high-pressure piping is required in the main shaft and haulage sections [19], [34].

Localised and micro-hydropower systems can easily be relocated and installed as they are modular systems suitable for both existing and new mines [12]. Localised and micro-hydropower systems use electric centrifugal or positive displacement hydro pumps to pressurise the incoming mine service water between 12 MPa and 18 MPa [12]. The hydro pumps, electric motors and ancillary equipment needed for their operation are referred to as hydropower packs or power packs. The power packs require an electrical and service water connection, the capacity of which is established by the requirements of the mine.

[13] Adapted from [33].

The power pack's specifications range from a 2.4 L/s, 55 kW micro set-up to a 9.6 L/s, 220 kW localised installation.[14] In a localised hydropower system, there is a localised hydropower pump station that supplies high-pressure water to a raise line with multiple active stoping panels and crews. The layout of a localised hydropower network and pump station is depicted in Figure 1-11.

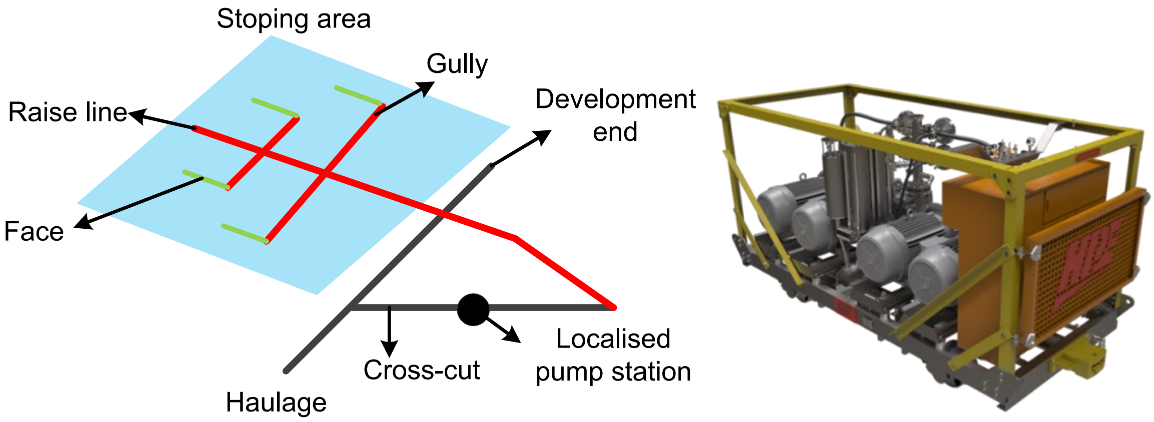

Figure 1-11: Localised pump station layout (left)[15] and HPE's localised rail-mounted pump station (right)[16]

A micro-hydropower system differs from localised hydropower in that they have smaller pumping capacities and generally only supply one stoping panel per system. Thus, the power packs are located closer to the active panel they supply. Micro-hydropower systems have the advantage of always operating at their optimum pressures and have been employed in a wide range of mines' development ends, creating a hybrid mining environment [19].

A development end in underground mining is an excavation of rock typically in the form of a tunnel that extends haulages.[17] The excavations allow for access to stoping regions where the ore bearing material is mined. Figure 1-11 shows the development end extending the haulage further, which allows for an additional cross-cut and raise line to be developed in the future. More recently, mines have been trialling micro-hydropower systems in their stope environments. The layout of a typical micro-hydropower panel layout is depicted in Figure 1-12.

[14] HPE SA. (n.d.). High pressure pump. Retrieved August 7, 2022, from https://www.hpesa.com/product/power-pack/

[15] Adapted from [35].

[16] HPE SA. (n.d.). High pressure pump. Retrieved July 5, 2023, from https://www.hpesa.com/product/power-pack/

[17] Britannica. (n.d.). Underground mining. Retrieved August 16, 2023, from https://www.britannica.com/technology/mining/Underground-mining

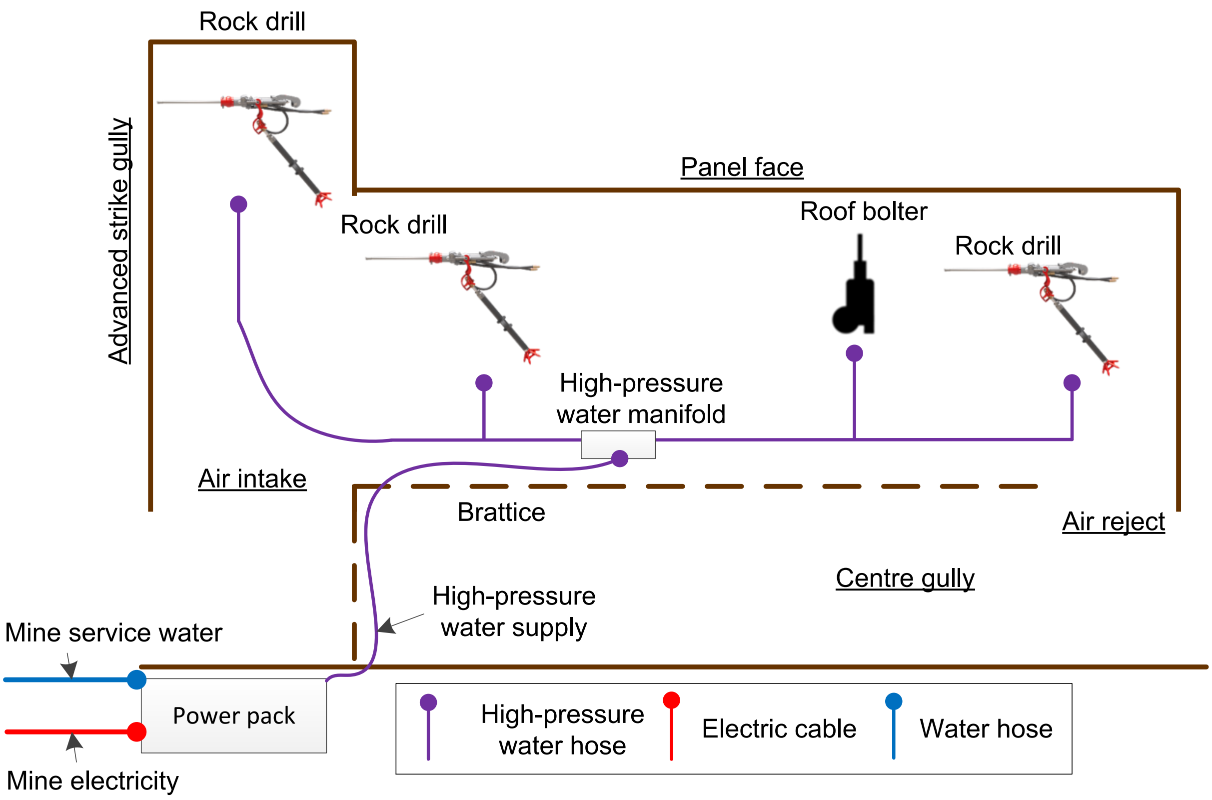

Figure 1-12: Typical hydropower stope layout[18]

The stope layout in Figure 1-12 differs from other alternative and conventional technologies. There is only one high-pressure water supply hose running into the panel and all the drills are supplied from a common manifold. The hydropower power pack is situated near the panel and is supplied by the mine with service water and electricity. For a typical stoping crew, one micro 55 kW power pack is needed to operate four drills; therefore, an additional 55 kW of electrical heat load is added to the stope environment.

Hydropower systems do, however, have a higher instantaneous water consumption than their compressed-air alternatives [22]. The water consumption of hydropowered systems typically varies between 0.64 L/s and 1 L/s, taking the latest hydropower drilling solutions available in South Africa into account. Whereas the widely used S215 compressed-air-powered drill typically consumes between 0.12 L/s and 0.22 L/s. From this, the instantaneous water consumption will be higher for the hydropower solutions. Hydropower drills use water in two distinct ways, namely in rotation and percussion of the drill steel (70%) and in flushing of the drilled hole (30%) [35].

[18] Illustration by author.

Some hydropower systems recirculate the water being used for rotation and percussion by connecting dump hoses to the outlets/exhausts of compatible drills. The water in the dump hoses is gravity-fed into a collection tank at the bottom of the stope. The water from this tank is pumped back to the service water inlet for the hydropower power packs to be used again. The recirculation of hydropower water reduces the dewatering volume of the drills since only 30% of the water is dumped onto the footwall of the stope. This reduces water demand, resulting in less pumping energy required for dewatering the mine [35].

Fraser [35] states that 100% of the service water cannot be recirculated as this will lead to salt and heat build-up [16]. The recirculated water will also increase in temperature from frictional heat originating from the pump and drill mechanism [36].

Hydropower systems have an overall system efficiency of 20%, which increases the available energy at the face compared with that of conventional compressed-air systems at 2–4% [12]. This reduces penetration times in comparison to compressed-air drilling at a supply pressure of 450 kPa [12]. Moving the energy source closer to the face reduces the line losses of the system, which, in turn, increases the system's overall efficiency.

The increase in system efficiency of hydropower in comparison to compressed air is further aided by the fact that high-pressure water leaks need to be managed better than compressed-air leaks [19]. Hydropower technology promotes a healthier working environment as there is no misting of carcinogenic oil in the stope environment [24].

1.4.4 Sources of heat

There are four main sources of heat in a conventional underground mine, namely heat radiation from the virgin rock, transportation of the ore, electromechanical equipment, and heat release from the adiabatic compression of the ventilation air [37]. A temperature increase of the local environment can decrease the production efficiency of labourers and cause serious harm in extreme cases [38].

Examples of high-temperature heat injuries are heat exhaustion, heat cramps and heatstroke [39]. The decrease in production efficiency of labourers is directly correlated to the temperature and velocity of the ventilation air. Figure 1-13 illustrates the relationship between labourers' production efficiency and the ambient wet-bulb temperature.

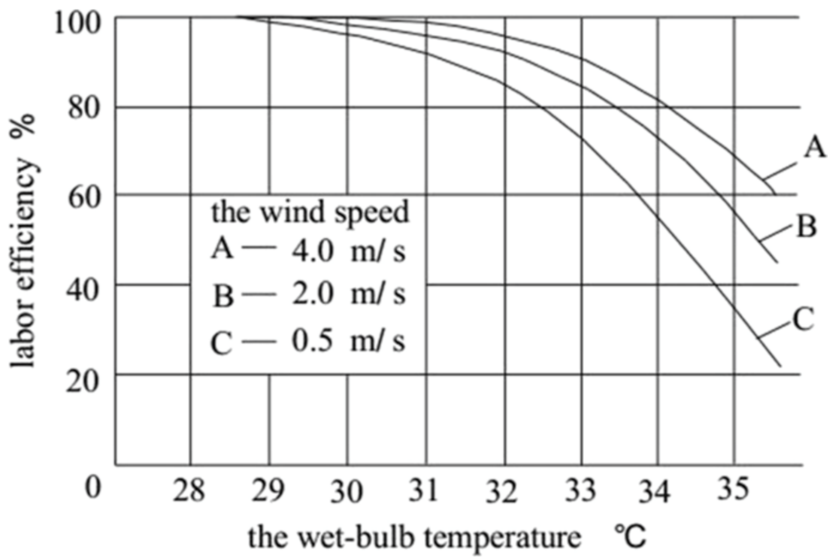

Figure 1-13: Production efficiency and temperature corelation [40]

It is clear from Figure 1-13 that the production efficiency of labourers decreases with an increase in the ambient wet-bulb temperature. Thermal stress exposure temperature limits are defined in the *Mine Health and Safety Act 29 of 1996* as a wet-bulb temperature of 32.5 °C and dry-bulb temperature of 37.0 °C. Workplaces exceeding these limits are deemed unsafe [41].

For a conventional compressed-air network, the heat rejected by centrifugal compressors on surface falls outside of the boundary of concern regarding heat management in a mine. However, moving electric motors or power packs into the local environment or within the boundary of concern can cause localised heating [19]. Localised heating is the result of heat rejection from electric motors, which is one of the main reasons for localised smaller compressors not being commonly used underground in conventional compressed-air networks [19]. Figure 1-14 illustrates the difference between compressors within and outside the boundary of concern and their respective heat rejection paths.

According to Clement [42], an additional 10 kW of heat will need to be removed from the stope environment if a pneumatic rock drill is replaced with a comparable hydraulic drill. Additionally, pneumatic rock drills are seen to cool the local environment due to the expansion of the compressed air. This cooling can equate to 5 kW, which the ventilation has to supply through the stope environment. Thus, an additional 15 kW of cooling may be required per drill if they were to be converted to a hydraulic system [42].

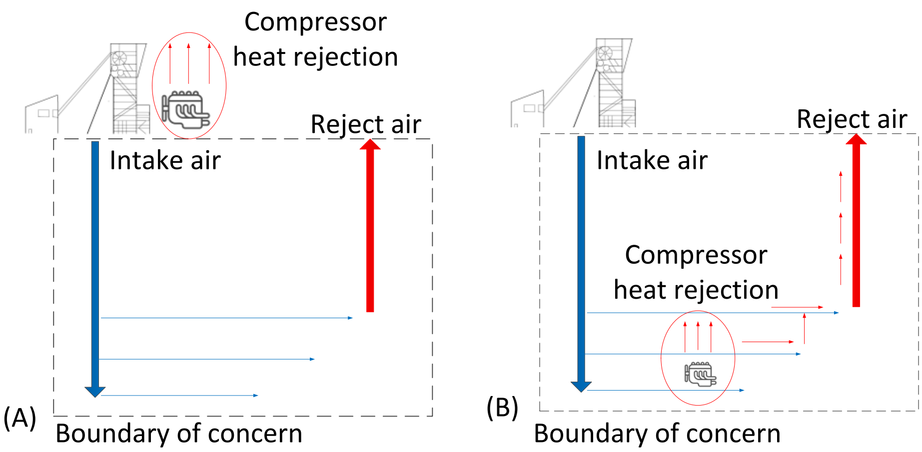

Figure 1-14: Heat boundary of concern in an underground mine[19]

When considering the electro-hydraulic, electric and micro-hydropower drilling alternatives discussed in Sections 1.4.1–1.4.3, it is important to note that these alternative drilling technologies introduce additional electrical heat load into the stope environment. This additional heat can have negative effects on the ambient conditions through localised heating and increase the risk of heat injuries if not considered properly.

1.4.5 Comparison of alternative drilling technologies

This section summarises the electrical heat load and environmental contaminants of the stope environment for each of the above-mentioned alternative drilling technologies. The aim of listing the environmental contaminants is to indicate possible health and safety concerns for each technology. Table 1-2 compares them with the conventional compressed-air drilling method.

Table 1-2: Alternative handheld drilling technologies comparison

KPI	Compressed air	Electro-hydraulic	Electric	Micro-hydropower
Water flow rate [L/s]	0.202 [22]	0.200 [28]	0.147 [22]	0.700[20]
Power [kW/drill]	–	10	2.2	13.75*
Local environmental contaminants	600 ml rock drill oil (4-hour drill time) [15]	Hydraulic oil	–	–
In-stope requirements	Compressed air and service water	Electrical supply and service water	Electrical supply and service water	Electrical supply and service water

*A 55 kW power pack can supply four drills

[19] Illustration by author.

[20] HPE SA. (n.d.). Handheld rock drill: HHH3. Retrieved July 5, 2023, from https://www.hpesa.com/product/hand-held-rock-drill-hhh3/

When comparing the different alternative handheld drilling technologies in Table 1-2, the micro-hydropower technologies have the highest instantaneous water flow rate. Additionally, micro-hydropower systems have the highest power requirement per drill compared with electric and electro-hydraulic systems. Therefore, micro-hydropower systems have the greatest risk of adding additional heat into the stope environment.

1.5 Mine ventilation simulation software

Mine ventilation networks are complex and difficult to manage; however, mine ventilation simulation software is used to manage these networks, which improves the level of ventilation management [43]. Ventilation simulations are further used to predict ventilation network characteristics, which is vital in mine ventilation planning, thus further improving the management of mine ventilation networks [44].

Various simulation software packages are used in ventilation modelling, including Vuma-3D, Process Toolbox and Ventsim [45], [46]. These three simulation packages use thermal-hydraulic solvers, which enable the determination of incompressible flow using thermodynamic principles and fluid dynamic properties [47], [48]. These thermal-hydraulic solver simulation packages can be used to model the stope environment and its respective heat sources. Therefore, enabling the prediction of ambient ventilation conditions in the stope environment and changes therein because of changing drilling technologies, as discussed in Section 1.4.4.

1.6 Need for the study

Considering the alternative drilling technologies in Section 1.4, it is clear that alternative drilling technologies have been developed to reduce the penetration rates of pneumatic rock drills and address their associated health and safety concerns. However, alternative drilling technologies add heat into the stope environment.

Additional heat in the stope environment will negatively affect the miner's productivity and can cause serious harm through heat injuries. Therefore, there is a need to investigate alternative drilling technologies and, specifically, their heat load impact on the stope environment.

1.7 Literature study

This section provides an overview of the most recent and relevant research related to the field of alternative handheld rock-drilling technologies. Keywords such as alternative drilling, handheld drilling, mine heat load, hydropower and more were populated in search engines such as ScienceDirect, Google Scholar and Scopus. Journals and other publications of the South African Institute of Mining and Metallurgy and similar bodies were reviewed along with relevant citations found therein. This was done to determine what has been covered in previous research and identify possible gaps in the research.

It is important to note that there are several studies where the authors of the articles are affiliated with alternative drilling technologies manufacturers. Care has been taken to view these studies objectively due to the inherent bias of the manufacturers.

The studies were evaluated against the following categories:

- Alternative drilling technologies: Whether the study compared alternative drilling technology with conventional drilling systems.
- Heat load: Possible heating or cooling aspects.
- Simulation: Use of simulation software to predict or evaluate heat load effects.

These categories were chosen to determine whether the heat addition of alternative drilling technologies have been investigated previously in literature and to determine the possible localised environmental effects of the increased heat load on the stope environment.

Additionally, the use of ventilation simulations was analysed in these studies to determine the use of simulations in heat load analysis and the requirements for a ventilation simulation. The comparison of these categories in combination with one another also indicates clear gaps in research and the importance thereof.

The studies that fall in the above-mentioned criteria are described in the following manner:

- Title of study.
- Author(s).
- Brief overview.
- Shortcomings and recommendations.

Experimental procedures, model accuracy and results are discussed where applicable.

1.7.1 Previous studies on alternative drilling technologies

A limited amount of research has been published on alternative drilling technologies in the South African mining context. However, the most relevant of these studies are provided as follows:

Study 1 (2016) [29]

Title: A new electro hydraulic hand held rock drill tested by Anglo American NMT

Authors: F. Fourie, P. Valicek, G. Krafft and D. Baird

Overview:

This study focused on the comparison between the electro-hydraulic HRD100 from Epiroc and the electric Hilti TE MD20. A trial between the two technologies was done and the HRD100 drill outperformed the Hilti TE MD20 in Anglo American's setting. A reduction in the collar-to-collar time and shift time was observed. Additionally, a cost analysis of pneumatic, electric, hydropower and electro-hydraulic technologies was done according to the mine's specific requirements. It was found that the total drill cost per panel per day for hydro and electro-hydraulic drills is cheaper than for pneumatic and electric drills.

Shortcomings and recommendations:

The trialling environment and thus heat load implications of the HRD100 and Hilti TE MD20 were not investigated in the trial.

Study 2 (2008) [18]

Title: Development and implementation of an electrically powered stope rock drill for Tau Tona mine

Authors: A. van Jaarsveld, S. Ebben and AngloGold Ashanti

Overview:

This paper focuses on the development and implementation of the Hilti electric handheld rock drill in a joint venture with AngloGold. The reasons for the investigation were to improve cost control, working conditions, face advance rates and the safety of ageing pneumatic handheld rock drill technology. The inherent inefficiencies of growing water reticulation and compressed-air networks and the associated maintenance costs were noted as a major reason for the investigation into alternative drilling technologies.

Hydropower drilling technology was reviewed but was ultimately not considered due to the high costs of implementation and possibly dangerous consequences from supply line failures. The paper outlines the steps followed by Hilti and AngloGold in the development of a suitable underground handheld rock drill from prototype to operational versions. The paper further outlines the logistics and preparations needed for a new drilling technology to be tested in the field. To prepare for the trials, a crew, overseer and manager have to be selected for the duration of the trials. The crew need to be trained on the new drill technology and the operational procedures prepared. A workplace with suitable electrical, water and compressed-air reticulation needs to be selected and prepared. Additionally, all support infrastructure and systems have to be prepared.

This paper outlines all the complex systems that have to work with one another for a trial to be successful. The paper describes the difficulties of trialling different drilling technologies and compares them since the performance of the technology is directly related to corporate policies, contract agreements and local circumstances. As stated in the paper, “each intended application is likely to arrive at a different conclusion”, which highlights the difficulties in running and comparing two trials. The paper proceeds to explain the results of the first trial of the new technology at the AngloGold’s Kopanang site.

The main takeaways from this trial were that the drill time of the Hilti electric drill was longer than the S215 pneumatic rock drill and that Hilti overall reduced the cost per metre drilled. The trials of the Hilti electric rock drill continued from 2002 until February 2006 when 236 drills were rolled out for use on the Tau Tona gold mine on a lease basis from Hilti.

Shortcomings and recommendations:

The Hilti trial on the Tau Tona gold mine was a success due to the poor compressed-air reticulation on this mine in particular. The reason for the failure on the initial trial sites was due to electric drills having a slower penetration rate than the existing pneumatic drills. A shortcoming of this paper is the relative cost comparison between developing and implementing the new electric handheld rock drills versus upgrading the existing compressed-air network to meet the requirements of the S215 pneumatic rock drills. This would have been an interesting comparison; however, the electric rock drill nonetheless improves on the noise-related hazards associated with pneumatic rock drills. The paper also did not consider electro-hydraulic drilling technology in its comparison before choosing to develop the electric rock drill. The operational requirements of this technology would be similar to those of electric rock drills. The heat load in the stope was also not addressed in the study.

Study 3 (2014) [24]

Title: Hydropower: A mature, game-changing technology

Author: P.D. Fraser

Overview:

The paper focuses on showcasing the ability of hydropower technology through seven case studies. Each case study demonstrates a different capability of the technology and how it can improve or replace existing mining methods. The seven case studies cover hydro-stoping with handheld rock drills, drilling of ore passes, box front systems, flat-end development, raise development with a monorail rig, reef boring, and energy recovery through pumping systems.

The handheld rock drill case study illustrates the success that hydropower drilling technology has had on six active mines where HPE drills are used in roof bolting, raise development and stope drilling. The success is directly related to the performance of the hydropower drill. The paper states that hydropower drills are 2.8 to 3.75 times more powerful than worn pneumatic drills at 4.5 bar. The hydro drills further boast increased torque compared with the pneumatic drill and reduced water consumption per tonne of rock mined.

The reduction is due to two factors. Firstly, the auto water shut-off of the drills where water is only used while percussing. Secondly, hydropower drills recirculate 70% of the service water used while drilling. Due to the recirculation, only 30% of the total drill demand is required from the mine's service water, which substantially reduces the drills' instantaneous water consumption. The paper details that the capital cost required for a localised hydropower system is 20% to 30% less than a pneumatic system when the capital cost of compressors is included. A list of benefits of hydropower technology is stated. The key benefits that are not always highlighted are listed here:

- Improved safety due to reduced drill operator time at the face.
- Reduced water usage with recirculation.

- Healthier working environment – no carcinogenic oil mist or fogging.
- Cooler working environments when chilled hydropower water is used to add positional cooling into the mine.

The paper concludes by stating that hydropower offers new game-changing opportunities in both new, smaller mines and existing mines where new areas need to be opened.

Shortcomings and recommendations:

The paper states that cooler working environments are achieved by using chilled hydropower service water. However, chilled service water cools the stope environment in conventional stopes through the same mechanisms. The additional heat load of the hydropower drill needs to be determined to quantify the effect of the technology on the environment. This paper does not determine the heat load effect and only comments on the cooling added by using chilled service water.

Study 4 (2006) [32]

Title: Electric rock drilling system for in-stope mining in platinum operations

Author: P.J. Petit

Overview:

This study focuses on the performance comparison between standard pneumatic drilling solutions and results from ongoing electric rock drill trials. Trials were conducted at Hackney, Amandelbult and Brakspruit. The drills were tested on the UG2 platinum reef band. The electric rock drills were evaluated on several production, technical performance, safety, health and environment key performance indicators (KPIs).

The results of the trials demonstrated that the drilling cycle is affected by multiple factors, including the penetration rate, length of the hole and the experience of rock drill operators. Their experience affects the penetration times of the drill due to the linear relationship between the contact pressure or feed force of the drill and the penetration rate. Performance data from the trials were analysed; however, due to uncontrollable factors, erratic and insufficient information and the diverse geology of the mining operations, the author could not establish any trends from the trials. This highlights one of the inherent issues with trialling equipment on varying mines.

Shortcomings and recommendations:

This study highlighted the inherent issues of trialling drilling equipment with a set of KPIs and the inefficiencies of receiving reliable performance data. However, the added electrical heat of the electric rock drills was not evaluated.

Study 5 (2010) [35]

Title: Hydropower technology can assist in meeting the safety and health '2013 milestones' and save energy: A case for 'localized' hydropower systems in general and hydropowered stope drill rigs in particular

Author: P.D. Fraser

Overview:

This study focuses on the implementation of localised hydropower systems and their impact on existing mines. Through the use of positive displacement pumps, mine service water at the level or cross-cut entrance is pressurised to around 18 MPa. This high-pressure water is used to power the hydro drills in the stope environment.

The study states that with recirculation of the hydro-drill discharge water, hydropower systems use less energy and water than standard pneumatic drill systems. Up to 70% of the service water supplied to each drill can be recirculated in a closed system, thus reducing the dewatering volume, pumping energy and required water supply of the stope. It is noted, however, that 100% of the service water cannot be recirculated as it will result in salt and heat build-up on the level.

Shortcomings and recommendations:

The study mentions that 100% recirculation of the mine service water will result in heat build-up in the level. However, there is no mention of the heat load in the stope environment with the introduction of the localised hydropower system and any additional effect that recirculation of service water up to 70% may have on the localised environment.

Study 6 (2010) [22]

Title: The energy and water required to drill a hole

Author: P.D. Fraser

Overview:

This study compares the energy demand of compressed-air, hydropower and electric handheld rock drills to drill a hole in the underground South African mining environment. The kilowatt-hour per metre drilled and the tonnes of water per tonnes of rock intensity of each technology were calculated and compared. The drilling times and water consumption of the drills were calculated based on typical performance figures for the technologies and based on the same stoping configuration.

Worst-, middle- and best-case performance scenarios were calculated for each technology to create a range of operations for the respective technologies. The power needed to generate compressed air, drill penetration rates, drill energy/motive powers, dewatering efficiency for a range of pumping heads and necessary refrigeration energy was calculated.

In conclusion, compressed air uses significantly more energy than hydropower and electric rock drills. Localised hydropower was seen to consume the least amount of water if on-level recirculation is used with the energy usage of electric and hydropower drills being comparable to one another.

Shortcomings and recommendations:

The refrigeration energy investigated was the energy required to cool the service water used by the drills; however, the heat load effect of the drills in the localised stope was not compared or discussed. The varying technologies will have different localised effects on the environment. Hydropower technology needs to use in-stope water recirculation to be comparable to electric rock drills. However, as stated previously, the heat load effect is not investigated.

Study 7 (2008) [19]

Title: Hydro power and stope drilling systems: An energy-saving perspective

Author: J. Wills

Overview:

This study compares the cost and energy implications of pneumatic systems, gravity hydropower systems, pumped hydropower systems and electric drilling systems considering the South African electricity crisis. In efforts to reduce power consumption on mines by 10%, the study discusses the possible impact that implementing alternative drilling solutions may have on a mine's overall energy consumption. The considerable energy consumption in pneumatically powered mines comes largely from the management of the compressed-air system, leaks, line losses and misuse of the resource.

The power-to-mass ratio of the four systems was compared with hydropower being significantly more powerful in that regard. When looking at the energy efficiency of the drills, it is seen that pneumatic drills are energy efficient with electric drills' efficiency being relatively similar. Hydropower drills are seen to be less energy efficient and consume more power per metre drilled. However, when the total system is considered and the line losses of the compressed-air network are accounted for, the pneumatic drills system's efficiency per metre drilled drops substantially.

Hydropower systems are not as efficient per metre drilled than electric drills; however, compared with pneumatic systems, there is still a large increase in efficiency. Thus, there is still a significant cost-saving opportunity with the benefit of improved drill performance. Compressed-air systems can be made more energy efficient by reducing the length of the compressed-air reticulation network. Compressors underground can cause localised heating due to the heat rejection in the mine; thus, it is uncommon to see compressors underground.

Shortcomings and recommendations:

The study mentions the localised heating that underground compressors can cause; however, there was no investigation into the stope heat load and the impact that hydropower or electric systems may have on the localised heat load. Similar to the argument against localised smaller compressors, the power packs of the localised hydropower systems have to be located in the mining environment whereby the heat rejection of the motors needs to be considered.

Study 8 (2008) [12]

Title: Saving energy by replacing compressed air with localized hydropower systems: A 'half level' model approach

Author: P.D. Fraser

Overview:

This paper outlines the general South African underground mining environment and their use of compressed-air rock drills. The proportion of compressed-air generation costs for a typical gold and platinum mine is stated at between 20% and 40%. From this, the use of localised hydropower systems is explored as a replacement for traditional compressed-air systems in all areas of the mine. The paper discusses the application and advantages of hydropower systems in various categories, including energy efficiency, water consumption and management, and reticulation options.

The energy efficiency of the hydropower, oil electro-hydraulic and electric drills is shown to be significantly higher than traditional compressed-air systems. Regarding water consumption and management, hydropower drills are demonstrated to have two times the overall water consumption over the duration of a shift. However, when comparing the total energy usage of systems, hydropower and electric drilling is seen to have a 90% and 96% relative energy saving compared with compressed air when the input drilling energy and dewatering pump energy are considered.

Shortcomings and recommendations:

The paper mentions that electric drills add heat to the local environment, whereas hydropower drills can cool it. Yet, the paper does not elaborate on the heat load of either technology or how the hydropower drills may cool the localised environment.

Study 9 (2013) [34]

Study 9 introduces aqua power-drilling technology in their comparison between conventional pneumatic, electric and hydropower handheld rock drills. Aqua power differs from localised hydropower systems where there are individual smaller capacity power packs for each handheld rock drill. Localised hydropower will have a larger capacity power pack capable of powering multiple hydropower drills at one time. Aqua power operates similarly to electro-hydraulic systems as seen in Figure 1-7, whereby each drill is powered by an individual power pack although water is used instead of oil. The water is circulated under high pressure in the closed loop system to power a handheld rock drill or ancillary hydro equipment up to 1 L/s.

Title: What is the best energy-delivery system for hand-held stope drilling and associated equipment in narrow-reef hard rock mines?

Authors: P.J. Petit and P.D. Fraser

Overview:

The paper evaluates alternative handheld rock drills in narrow-reef hard rock mines. The conventional pneumatic drilling solution is compared with electric handheld rock drills, hydropower handheld rock drills and aqua power handheld rock drills in the stope environment. An analytic hierarchical process was followed to evaluate each of the alternative drilling solutions in a decision matrix. The decision matrix included the following headings: operating costs; capital expenditure; overall electrical consumption and cost; legislative requirements; safety, health and environment; technical penetration rate; implementation; and management and business risk.

The performance matrix and ranking of the alternative drilling technologies were formulated from the results of a survey given to techno-financial analysts, consultants, operation, production managers and suppliers, who were all classified as expert professionals in their field. The performance matrix resulted in hydropower drilling being the preferred overall solution. However, it fell short of pneumatic technology in the implementation and management criteria as conventional pneumatic drilling technology is widespread across the industry.

Shortcomings and recommendations:

This paper did not consider electro-hydraulic technology in its comparisons and there is no mention of heat load in the stope. More information regarding the safety, health and environment criteria could have been given to elaborate on what was being assessed and whether any heat load factors were investigated.

1.7.2 Previous studies performed on the heat load in a stope environment

Evaluating the heat load of alternative drilling technologies in the stope environment would allow mines to understand the localised effect thereof as any effects on the localised dry-bulb and wet-bulb temperatures may result in possible changes to the ventilation and water controls.

Study 10 (2015) [36]

Title: Potential sources of heat in underground mines: A review

Authors: T. Maurya, K. Karena, H. Vardhan, M. Aruna and M. G. Raj

Overview:

This paper provides an overview of the potential sources of heat in an underground mine. These sources include but are not limited to the geothermal gradient, autocompression of air, mechanised equipment, explosives and blasting, and mechanical processes and lights. Pneumatic drills have two opposing effects on the localised heat load. Firstly, there is frictional heat from the machine as it is performing work. Secondly, however, there is also a reduction in the temperature of the air exhausting from the machine due to the removal of energy from the compressed air.

Alternative drilling technologies result in additional electrical equipment being required underground, with its heat rejection being directly proportional to the equipment's efficiency. The machine's efficiency also determines the distribution of the heat produced. Although a motor with a better efficiency will produce less heat at the motor and transmission, more heat will be produced at the delivery/pick-point of the system. Underground fissure water and service water is a further source of heat in a mines. The water gets heated from the surrounding rock and transfers its heat to the mine air through evaporation, which increases the latent heat.

Shortcomings and recommendations:

Where the greater efficiency of alternative drilling technologies is concerned, there will be more energy available at the face of the stope than that of traditional pneumatic systems. The energy imparted to the stope through the energy medium needs to be quantified. This increase in energy at the face increases the heat load in the stope mainly through higher exhaust water temperatures. Additionally, with hydropower technologies, there is an increase in instantaneous water consumption in the stope.

The combination of increased water consumption and higher water temperatures in the stope needs to be investigated. The study also did not indicate the effect that chilled service water may have on the heat load of the mine in the stope environment.

Study 11 (2020) [46]

Title: Practical determination of heat loads for existing deep level gold mines

Author: D. Nell

Overview:

This thesis explores and develops a method to determine the heat load in an existing deep-level gold mine. An energy balance is created from the various sources of heat entering and leaving a mine. The heat sources entering the mine include geothermal, water, electricity, fuel, people, ventilation air, compressed air, strata movement oxidation and explosives. The various energy sources are balanced according to the conservation of energy law. The sources of energy leaving the mine include rock hoisted, ventilation air and water pumped.

The method is determined on a steady-state basis due to the dynamic nature of the mine system. The developed heat load calculation methodology has seven steps, namely: boundary definition, calculation of heat sinks, calculation of heat sources, calculation of geothermal heat, validation of the geothermal heat, evaluation of cooling surplus/shortage and, finally, evaluation of the seasonal impact. This method was evaluated in three case studies and the results of the method closely resembled that of a calibrated ventilation simulation model. Three thermal-hydraulic simulation packages, namely Vuma3D, Process Toolbox and Ventsim, were evaluated and compared. Process Toolbox was chosen as it can integrate mine cooling and ventilation systems.

Shortcomings and recommendations:

This method can be used to determine the heat load in the stope environment by adapting the boundary definitions of the method to a stope environment. The heat load of alternative drilling technologies can thus be determined using the steps in this methodology.

1.7.3 Previous studies performed on simulation of the stope environment

Studies relating to stope ventilation simulations and the prediction of heat load effects in the stope environment were evaluated. The simulation methodologies used were also evaluated in order to adapt or create a stope ventilation simulation from which the stope heat load could be characterised and predicted for changing drilling technologies.

Study 12 (2002) [49]

Title:	Numerical modelling of heat flow in mines
Authors:	F.H. von Glehn, R. Hemp and R.C. Funnell

Overview:

This study discusses the developments in simulations of heat flow models that focus on underground stopes and dams. The heat liberated in the stope environment is one of the main contributors to the overall mine heat load. To combat this, most deep-level mines in South Africa use chilled service water to provide cooling in the localised stope environment. Exposed chilled service water cools the ventilation air and the surrounding rock it contacts.

It was noted that in stopes with higher water flow rate instances, the temperature of the water leaving the stope can be significantly lower than that of the wet-bulb air temperature exiting the stope. Therefore, the resource is not used as effectively as lower flow rate instances. Here, the water on the footwall has more contact time with the ventilation air and can cool the ventilation, which has a better cooling efficiency.

A new procedure was developed to quantify the transient cooling effects of using chilled service water in stopes. The analytical model incorporates two heat models, namely the rock heat model and the general stope model. The rock heat model uses a computational fluid dynamics (CFD) package to carry out the finite-difference analysis to determine the predicted rock temperatures around a stope with an advancing face.

The general stope model is used to predict the local air temperature conditions in the stope and the temperature of the service water leaving the stope. This model sums up the main sources of heat in the stope and integrates the heat loads over the length of the stope. The main sources of heat used include exposed rock, broken rock, fissure water, backfill material and machines. The model was validated using data obtained from underground field trials and the results had acceptable accuracy. The model used was an iterative spreadsheet model.

Shortcomings and recommendations:

The study focused on the transient heat load in a stope over a mining cycle to determine the optimum stope cooling strategy. However, the heat load differences between conventional pneumatic drilling and hydropower drilling were not explored and the results of the cooling strategy were not given. A commercial CFD simulation package and an iterative spreadsheet model were used for the analysis.

Study 13 (2018) [47]

Title: Evaluating complex mine ventilation operational changes through simulations

Authors: A. J. H. Nel, J. C. Vosloo and M. J. Mathews

Overview:

This study investigated the optimisation of mine ventilation networks through simulation. A method was developed to analyse mine ventilation operational changes in a scalable manner. This method was evaluated on a case study mine with both operational energy cost and service delivery improvements seen.

The method steps include identifying the operational change in the ventilation network, benchmarking the service delivery system, acquiring available data, verifying data, establishing

KPIs to be assessed, evaluating available simulation packages, determining the simulation boundaries, creating and calibrating the simulation model, analysing results, and evaluating the operational change according to the selected KPIs. The simulation software Vuma3D was used as it was already available on the case study mine. The software is a thermal-hydraulic solver designed to model complex mine ventilation networks.

Shortcomings and recommendations:

The scalable nature of this method enables it to be applied in a stope environment. Thus, it can be used to create a simulation and evaluate the ambient conditions of varying operational changes in the stope. Vuma3D was used for the analysis.

Study 14 (2013) [50]

Title: Optimization of parameters to improve ventilation in underground mine working using CFD

Author: V. Chauhan

Overview:

This thesis evaluated the optimum brattice location in a T-shaped cross-cut region. CFD was used to simulate the cross-cut region and optimisation algorithms were used to maximise the airflow in the dead end of the T-shaped cross-cut. The method had four steps, namely problem identification, preprocessing, solution and post-processing. The CFD simulation and optimisation algorithms were able to establish the optimum brattice position and dimensions of the brattice. Ansys Fluent software solver was used for the CFD modelling of the T-shaped cross-cut.

Shortcomings and recommendations:

The method is adequate for determining and evaluating air velocity and pressure distribution in the T-shaped panel. However, the effects on the panels ambient conditions were not considered. Thus, the heat load and the changes in the heat load in the T-shaped panel were not determined. Ansys Fluent was the CFD modelling software used.

Study 15 (2018) [51]

Title: Mine ventilation characterisation through simulations

Author: A.J.H. Nel

Overview:

This study emphasises the importance of simulation in the life of mine (LOM) planning of mines, which includes factors such as ventilation and hoisting/primary access systems. By identifying that outdated methods were used to determine the LOM requirements, an integrated simulation methodology was developed to include ventilation networks and primary access in LOM planning. The methodology described included five main steps with sub-steps for each. These are LOM planned production rate, hoisting capacity, ventilation, simulation cost analysis, and approve the LOM plan.

A simulation may be required to determine the hoisting capacity and ventilation; however, a thermal-hydraulic solver is needed to simulate wet-bulb temperatures. The author states that Ventsim, Process Toolbox and Vuma3D are typically used simulation packages that incorporate thermal-hydraulic solvers. For the simulations, data is acquired either through the supervisory control and data acquisition system or manual measurements. From the verified data, a simulation model is to be constructed and calibrated iteratively. The author states that an error of lower than 10% is acceptable for the mining industry. The simulations, once calibrated, are used to analyse the LOM planning with the identified KPIs. The study goes on to investigate LOM scenarios in a case study by applying the above method.

Shortcomings and recommendations:

The study focuses on the larger boundary of concern regarding mine ventilation systems. Although it comments on the addition of heat due to additional hoists, it does not state the heat load effect of such additions. The methodology followed can be applied to smaller boundaries of concern such as the stope environment. The thermal-hydraulic solvers Ventsim, Process Toolbox and Vuma3D were identified as possible simulation packages.

1.8 Analysis of the literature study

Table 1-3 compares and summarises the 15 studies discussed above and highlights the gap in the literature.

Table 1-3: State-of-the-art matrix indicating gaps in past studies

Source	Alternative drilling technologies	Stope heat load	Simulation	Focus
Study 1 Fourie et al. (2016) [29]				Electro-hydraulic vs electric
Study 2 Van Jaarsveld et al. (2008) [18]				Electrically powered stope
Study 3 Fraser (2014) [24]				Hydropower technology
Study 4 Petit (2006) [32]				Electric rock drilling
Study 5 Fraser (2010) [35]				Recirculation energy implications
Study 6 Fraser (2010) [22]				Energy and water requirements
Study 7 Wills (2008) [19]				Hydropower, energy
Study 8 Fraser (2008) [12]				Localised hydropower systems
Study 9 Petit et al. (2013) [34]				Energy-delivery systems
Study 10 Maurya et al. (2015) [36]				Sources of heat
Study 11 Nell (2020) [46]				Mining heat load
Study 12 Von Glehn et al. (2002) [49]				Chilled water in stopes
Study 13 Nel (2018) [47]				Mining ventilation
Study 14 Chauhan (2013) [50]				Stope ventilation flow
Study 15 Nel et al. (2018) [51]				Mining ventilation

Key: Not in the scope of the reference | Included in the scope of the reference

From Table 1-3 it is clear that there is a gap in the literature where the heat load of alternative drilling technologies in the stope environment, aided by simulations, is largely undetermined. The studies that describe the development of a mine ventilation simulation model and heat load simulation model are shown in Table 1-4.

Table 1-4: Development of simulation methodologies

Study	Simulation software identified	Focus
Study 11	Ventsim, Vuma3D, Process Toolbox	Heat load
Study 12	Commercial CFD, Iterative spreadsheet	Heat load
Study 13	Vuma3D	Ventilation
Study 15	Ventsim, Vuma3D, Process Toolbox	Ventilation

These simulation methodologies can be used to create a combined ventilation simulation model of the stope environment in which the heat load is accounted for. The basic key simulation model steps identified in each of the simulation methodologies are as follows:

- Gather data.
- Construct model.
- Calibrate and verify the model.
- Apply the model.

1.9 Problem statement

From the investigation into conventional underground mining practices and handheld drills, it was determined that there are inherent problems with extensive underground compressed-air networks that are negatively affecting the performance of compressed-air rock drills. Compressed-air rock drills also introduce health and safety concerns into the stope environment through atomised oil particles.

Alternative drilling technologies have been developed to address the inefficiencies of compressed-air networks and health concerns of rock drills; however, these technologies add heat into the stope environment and the effect thereof is largely undetermined in the literature.

1.10 Aim and study objectives

From the three main alternative drilling technologies discussed, micro-hydropower has the highest potential of adding additional heat into the stope environment due to its high kW/drill electrical load in the stope. Additional heat in the stope environment will reduce miners' productivity and increase their risk of heat injuries if left unaccounted for.

Therefore, the aim of the study is to quantify the heat load of micro-hydropower technologies in stope environments. The following study objectives are outlined to achieve this aim:

1. Simulate the heat load characteristics of a stope environment.
   1.1. Quantify heat added/removed from the environment.
   1.2. Compare and validate simulation results to a real-world stope environment.
2. Predict thermal changes when introducing micro-hydropower technologies.
   2.1. Determine effect of the heat addition/removal on the stope environment conditions.
   2.2. Analysis of the environmental effect if multiple stopes are converted.

1.11 Study outline

A case study research methodology is applied in this study as it is utilised to develop a comprehensive understanding of a complex issue in its real-life context [52], [53]. Although it has been used extensively in social research, its application has been expanded to several social sciences disciplines and design research [54], [55]. A high-level summary of a case study methodology is shown in Figure 1-15.

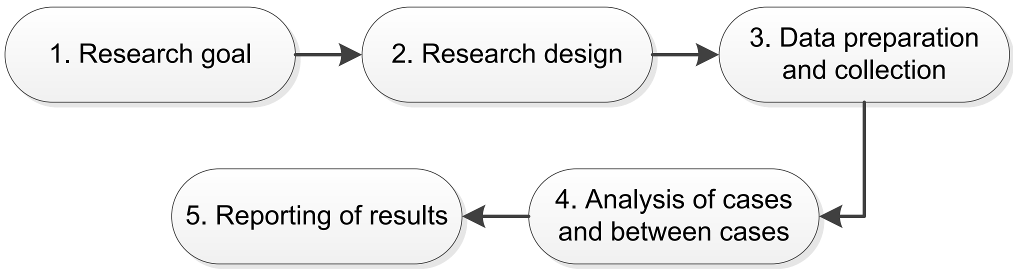

Figure 1-15: Case study research methodology (adopted from [56])

Each step of the case study research methodology is applied in the different chapters throughout this study. A summary of each chapter is provided below.

Chapter 1

This chapter served as an introduction to, and definition of the study goal, by following Step 1 of the case study research methodology. It provided an overview of conventional and alternative handheld drilling technologies in South African underground mining. The varying technologies and heat load implications were discussed. An overview of the relevant literature relating to alternative drilling technologies and their heat load was given. From the challenges and shortcomings in the literature, the problem statement and need for the study were formulated. Finally, the study objectives were provided.

Chapter 2

Following the research goal definition and learnings from Chapter 1, this chapter outlines the research design. The chapter describes how a method was developed that aimed to achieve the study objectives. A stope heat load method was developed, which included quantifying the heat load in the stope. The application of this method will enable a comprehensive understanding of the stope's heat load and thermal characteristics when introducing micro-hydropower drilling technology.

Chapter 3

In Chapter 3, the developed stope heat load method of Chapter 2 was applied to a case study mine. This chapter describes how a conventional stope environment was converted to a micro-hydropower stope. The heat load characteristics were determined through simulation and verified using the developed method, following the data preparation and collection step of the case study research methodology. The results of the implemented solution strategy were analysed between the scenarios following Step 4 of the case study research methodology (analysis of cases). Finally, Step 5 of the case study research methodology was followed by reporting on the results of the micro-hydropowered stope's heat load changes.

Chapter 4

This chapter concludes the results of the study and compares the outcomes with the objectives stated in Chapter 1. This chapter addresses the problem statement and presents the main conclusions. Finally, recommendations for further studies are discussed.

CHAPTER 2 – A METHOD TO QUANTIFY STOPE HEAT LOADS

2.1 Preamble

Chapter 2 describes how a stope heat load method is developed to predict the thermal changes in a stope environment when implementing micro-hydropower technologies. Each step of the method is numbered. This numbering acts as a route map when the overall stope heat load method is presented in the form of a flow diagram in Section 2.4.

The method begins by investigating and characterising the operational environment by defining the physical aspects of the stope environment and its operating equipment. The required operational changes when implementing micro-hydropower technologies should also be identified, including adding a hydropower power pack and removing compressed-air drills from the stope environment.

Once the operational environment has been characterised fully, it should be benchmarked. Benchmarking of the operational environment generates a baseline for comparison after the operational changes have been implemented and enables the nett effect of the changes to be determined. The benchmarked data needs to be verified to ensure it is accurate and reliable. For the stope environment, ambient environmental conditions at the intake and reject of the panel, inlet water temperatures and reject water temperatures are crucial benchmarking parameters.

Thereafter, the KPIs for the case study should be determined. The KPIs are used to evaluate and determine the nett heat load effect of the operational changes on the stope environment. Thus, the ambient ventilation conditions at the reject of the stope are important KPIs for this case study as the reject ambient ventilation conditions are critical for evaluating the stope's heat load.

Using this information, simulation packages capable of simulating the operational environment are evaluated. The most applicable software package for the operational environment is selected to create a calibrated simulation model. Next, an operational change simulation needs to be created by implementing the identified operational changes in the calibrated simulation.

Upon implementation, the last step of the method is to evaluate the operational change simulation results against the identified KPIs. The evaluation aims to define the nett heat load effect between the benchmarked and operational change environments.

2.2 Method development

2.2.1 Step 1: Define operational environment

The case study takes place in the operational environment. Therefore, the operational environment needs to be defined to allow for a fair comparison of the case study environment and its findings. For this study, the operational environment is a conventional compressed-air stope. Figure 1-4 depicted the operational environment of a conventional compressed-air stope. This figure clearly defines the stope's dimensions, number of active drills, drill technology, and service water and compressed-air supplies entering the operational environment.

Operational changes, such as the ventilation network, may affect or impose constraints on the operational environment, thus the operational changes need to be identified [47]. The identification of operational inefficiencies may lead to the identification of operational changes as operational changes may be necessary to address the inefficiencies [45].

This study evaluates the operational change of converting the compressed-air stope into a micro-hydropowered stope. Therefore, the stope's operational environment will change by adding hydropower drills and a power pack and by removing compressed air and compressed-air drills.

2.2.2 Step 2: Benchmark system

Once the operational environment and operational changes have been identified, the operational environment needs to be benchmarked [57]. Benchmarking standardises the existing operating parameters, which allows for the calibration of a simulation model and relative comparison of environmental conditions when evaluating the operational changes. Benchmarking of the environment is done by collecting data on the environmental conditions of the stope and any factors that may influence the environment. The typical data to be recorded is depicted in Figure 2-1, established from [43] and [45].

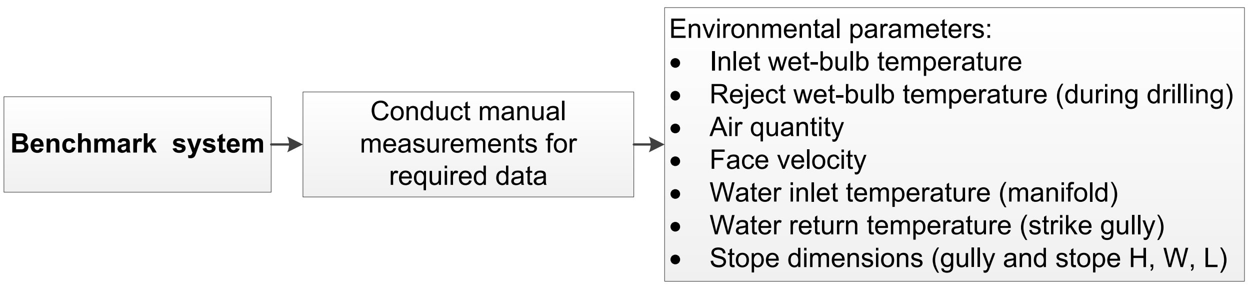

Figure 2-1: Environmental parameters to be benchmarked (adapted from [46], [47])

Manual measurements must be taken accurately as the degree of simulation accuracy is highly dependent on the source data [57]. The *Handbook on Mine Occupational Hygiene Measurements* describes the method for determining wet-bulb and dry-bulb temperatures using a whirling hygrometer [38]. An ordinary whirling hygrometer is illustrated in Figure 2-2.

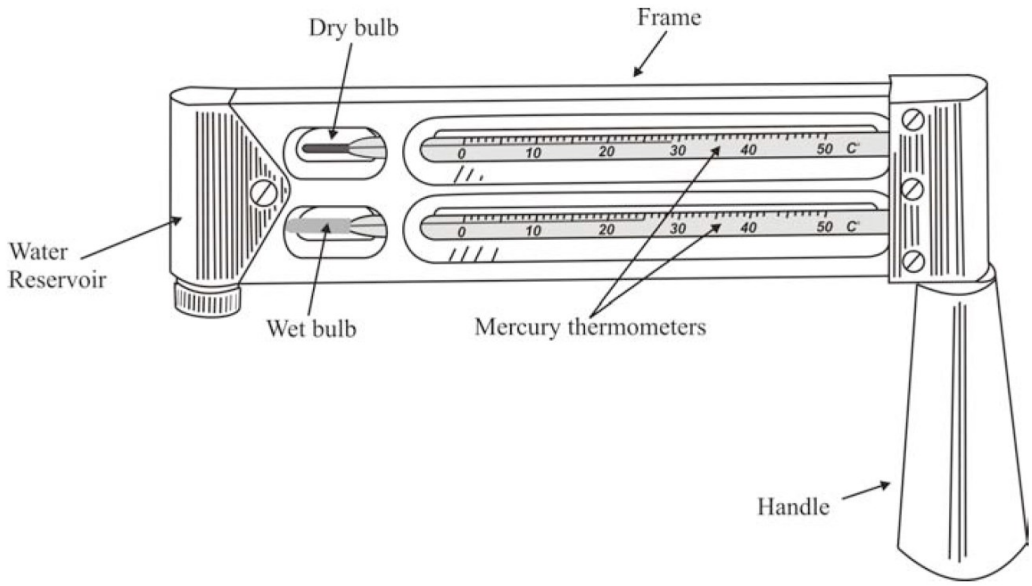

Figure 2-2: Ordinary whirling hygrometer [38]

Similarly, the *Handbook on Mine Occupational Hygiene Measurements* describes the method for taking ventilation flow measurements using a rotating vane anemometer [38]. A mechanical vane anemometer is to be used when the air velocity is greater than 0.5 m/s and a Kestrel-type digital anemometer when the flow is greater than 0.3 m/s [38]. Figure 2-3 shows these anemometers.

Figure 2-3: Mechanical vane anemometer (left)[21] and Kestrel-type digital anemometer (right)[22]

[21] CSE. (n.d.). Davis anemometers. Retrieved July 17, 2023, from https://www.csecorporation.com/Product-Davis-Anemometers
[22] Elcometer. (n.d.). Elcometer 410 anemometer. Retrieved July 17, 2023, from https://www.elcometer.com/en/elcometer-410-anemometer.html

This study uses the above-mentioned methods and equipment to determine the ventilation flow and temperatures in the stope environment. The atmospheric pressure and area at the measurement point are required along with the flow velocity to determine the mass flow of the ventilation air. The *Handbook on Mine Occupational Hygiene Measurements* describes both the method for taking the barometric pressure and the method for measuring the cross-sectional area required for the ventilation measurements [38].

Thermometers or temperature sensors such as a Tinytag temperature logger can be used to determine the temperature of service water. Additionally, externally mounted ultrasonic flowmeters such as the portable ultrasonic flowmeter from Fuji Electric can be used to measure the water flow demand of the stope environment. Examples of these measuring equipment are shown in Figure 2-4.

Figure 2-4: Tinytag View 2 (left)[23] and Fuji Electric portable ultrasonic flowmeter (right)[24]

2.2.3 Step 3: Verify data

The measurements conducted according to the specified mine occupational hygiene measurement methods need to be verified. The measurements are verified iteratively in this stope heat load method by taking two or more measurements. If there is a difference of more than 5% between two measured values, further measurements should be taken until the readings are within 5% of each other [38]. Additionally, different measurement instruments can be used. If their measurements have a percentage difference of within 5% of each other, the data can be considered accurate [57].

[23] Gemini Data Loggers. (n.d.). Tinytag View 2. Retrieved July 6, 2023, from https://www.geminidataloggers.com/data-loggers/tinytag-view-2/tv-4510
[24] Fuji Electric. (n.d.). Ultrasonic flow meter portable: FSC. Retrieved July 6, 2023, from https://www.fujielectric.fr/en/product/portable-flow-fsc-ultrasonic-flowmeter

2.2.4 Step 4: Determine KPIs

KPIs need to be identified from the benchmarked system. These KPIs are used to validate the impact of the operational changes and are important factors in the evaluation of the simulation [57]. Underground conditions and operational efficiency are typically the main drivers behind operational changes; therefore, underground wet-bulb temperatures, air mass flow and air velocity are typical KPIs that should be considered depending on the operational change [57]. Boundaries for these KPIs should be identified as these will act as constraints in the simulation. The constraints act as limits for the simulation and can be defined by technical and/or operational factors [47].

With relation to the case study stope environment, KPIs that quantify the heat effect of the operational changes will be the reject ambient conditions of the stope environment. However, to quantify the heat, the amount of heat added/removed over the stope environment by the drilling technologies is also an important KPI. Boundaries for these KPIs can also be based on legislation for a safe working environment, such as minimum air velocities and maximum allowable wet-bulb temperatures.

2.2.5 Step 5: Quantify heat load

A heat load study focuses on identifying and accurately quantifying heat sources in an environment [58]. Due to the introduction of additional heat in the stope environment through the hydropowered drills, the heat added or removed from the stope environment is an important KPI in this study. A heat load study focuses on identifying and quantifying each source [46]. An energy balance using first principles is evaluated to quantify the heat load over the stope environment. The steps to be followed are outlined in Figure 2-5.

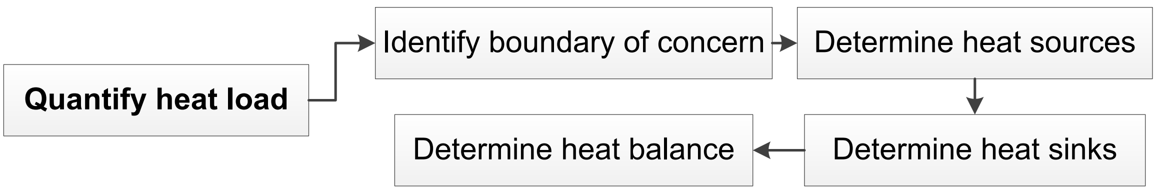

Figure 2-5: Heat load quantification method[25]

[25] Adapted from [46], [47].

2.2.5.1 *Identify boundary of concern*

Firstly, in the determination of the heat load, a clear boundary of concern needs to be identified. This boundary is needed to determine all the energy forms exiting and entering the area of concern at any time [46]. The boundary can range from an entire mine to a single workplace [46]. In this study, the boundary of concern focuses on the stope environment and the energy forms entering and exiting it. For a stope environment, these energy forms typically include service water, compressed air and ventilation air. Figure 2-6 depicts a simplified boundary of concern for a stope environment inclusive of a micro-hydropower drill system.

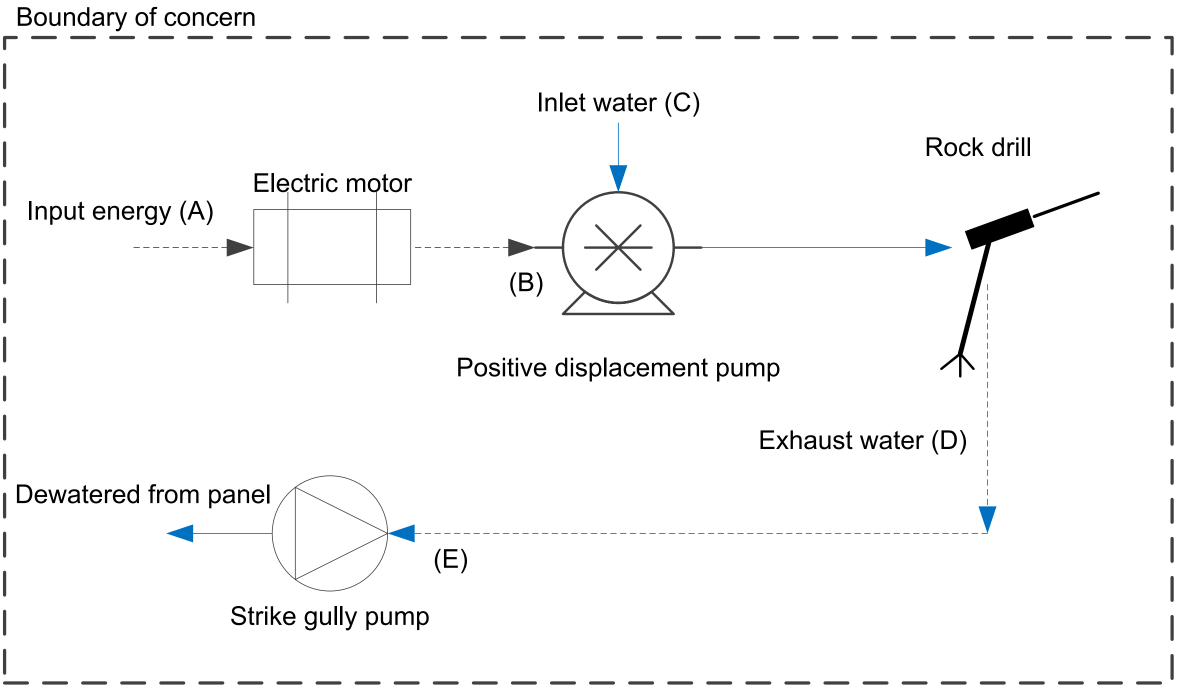

Figure 2-6: Simplified boundary of concern[26]

From Figure 2-6, the boundary of concern includes a hydropower power pack that requires an additional energy form (electricity) to enter the boundary of concern.

2.2.5.2 *Determine heat sources*

Once all the energy forms exiting and entering the boundary of concern have been identified, the heat sources within the boundary need to be determined [46]. There are various heat sources in the mining environment as seen in the literature. However, the main heat sources in the stope environment during a drilling shift are electrical equipment, fissure water and geothermal heat.

[26] Illustration by author.

However, geothermal heat is influenced by a vast number of parameters and is difficult to calculate [46]. For this study, the geothermal heat is determined by a heat balance of the heat sources and heat sinks.

Electrical energy is transferred into sensible heat in the mine if no potential energy is gained in the system [46]. Sensible heat is defined as the transfer of energy whereby no phase change takes place (increase in dry-bulb temperature), whereas latent heat is the transfer of energy to or from a system during phase change (increase in wet-bulb temperature).[27] Thus, the location of the heat source within the boundary of concern should also be considered since the heat may be added into intake airways, negatively affecting the upstream environment. In this study, the additional power pack in the stope environment acts as a heat source; however, the power pack does increase the potential energy of the water in the system.

The amount of heat transferred from the power pack to the water needs to be determined since the water is in direct contact with the stope environment and may act as a heat source. In a worst-case scenario, the total amount of heat added by the power pack is equal to that of the total rated electrical load. However, the power packs do not run at their maximum rating for the entire shift due to changing demands. By using the maximum water flow rate for each drill in the stope environment, the nett heat added to the water by the power pack can be determined by calculating the heat duty of the water, following Equation 2-1.

Equation 2-1: Heat duty [46]

$$Q = \dot{m}C_p(T_{out} - T_{in})$$

Where

Q	=	Heat duty	kW
$\dot{m}$	=	Mass flow	kg/s
C_p	=	Specific heat capacity	kj/kg · °C
T_{in}	=	Inlet water temperature	°C
T_{out}	=	Outlet water temperature	°C

Fissure water refers to water entering the mine uncontrollably through crevasses, faults, cracks or even from old mined-out areas [14]. In the stope environment, reject water from neighbouring active panels may also be considered fissure water if the water flows uncontrollably within the

[27] Madhusha. (2017, October 14). Difference between latent heat and sensible heat. *PEDIAA*. https://pediaa.com/difference-between-latent-heat-and-sensible-heat/

identified boundary of concern. The fissure water potentially has had a prolonged period of contact with the surrounding rock, resulting in increased water temperatures [46]. Therefore, the temperature of any water entering and exiting the boundary of concern should be measured to determine the heat added. Equation 2-1 is used to quantify this heat source. If there are multiple sources of fissure water, a weighted temperature is determined using Equation 2-2.

Equation 2-2: Flow-weighted temperature [46]

$$T_W = \frac{T_1\dot{m}_1 + T_2\dot{m}_2}{\dot{m}_T}$$

Where

T_W	=	Weighted inlet temperature	°C
$\dot{m}_T$	=	Total inlet mass flow	kg/s
T_1	=	Flow 1 temperature	°C
$\dot{m}_1$	=	Flow 1 mass flow	kg/s
T_2	=	Flow 2 temperature	°C
$\dot{m}_2$	=	Flow 2 mass flow	kg/s

2.2.5.3 Determine heat sinks

Similar to the heat sources in the boundary of concern, heat sinks extract heat from the environment [46]. As seen in the literature, there are three major heat sinks in mines, namely air-cooling power, secondary cooling and water-cooling duty [46].

With relation to the stope environment and quantification of the imparted heat, the service water used for drilling is the main heat sink in the stope environment. The inlet and reject water temperatures over the stope are used to determine the amount of heat removed by the water. By using the maximum water flow rate for each drill in the stope environment, the nett heat removed from the stope environment by the water is determined by using the heat duty formula given in Equation 2-1.

Similar to the heat transferred to the water, the amount of heat transferred to the air in the localised environment needs to be determined. The amount of heat in the air is characterised by the enthalpy of the air. Enthalpy is a measure of the heat content for both the dry air and the vapour present in the air.[28] The enthalpy of the air in the localised drill region before and during drilling is used to determine the amount of heat transferred into the air as the only change in the environment would be the introduction of the drills. The enthalpy is determined from the ambient environmental conditions (temperature, relative humidity and pressure). The localised zone around the drill, in which the ambient conditions of the air should be measured, is depicted in Figure 2-7.

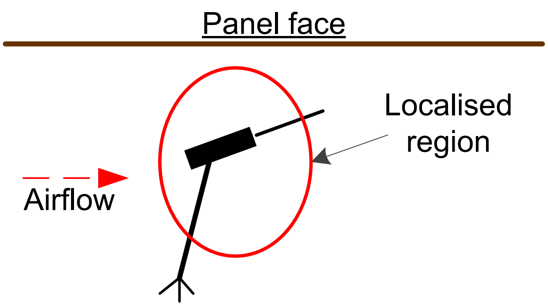

Figure 2-7: Localised drill region[29]

In order to determine the amount of heat transferred to or from the air during drilling from the drills, Equation 2-3 is used.

Equation 2-3: Air heat duty [46]

$$Q = \dot{m}(h_{During} - h_{Before})$$

Where

Q	=	Heat duty	kW
$\dot{m}$	=	Air mass flow	kg/s
h_{During}	=	Enthalpy of air during drilling	J/kg
h_{Before}	=	Enthalpy of air before drilling	J/kg

[28] HVAC Programs. (n.d.). What is enthalpy in an HVAC system? Retrieved August 15, 2023, from https://hvacprograms.net/enthalpy/#:~:text=What%20is%20the%20air%20enthalpy,Heat%20content%20of%20water%20vapor

[29] Illustration by author.

2.2.5.4 *Determine heat balance*

Once both the heat sinks and heat sources have been determined, the heat balance over the boundary of concern is determined using Equation 2-4.

Equation 2-4: Heat balance [46]

$$\text{Heat balance} = \text{Heat sinks} + \text{Heat sources} + \text{Remainder}$$

The remainder of the heat balance is attributed to heat gain from the surrounding rock/geothermal heat within the boundary. For this study, the geothermal heat is determined from the heat picked up in the wastewater from the drills before being dewatered from the stope environment. Thereafter, the heat load of the stope environment is concluded and quantified.

2.2.6 Step 6: Evaluate simulation packages

Based on the study objective of simulating the heat load characteristics of a stope environment, a simulation package needs to be selected accordingly. As discussed in the Section 1.7.3, a thermal-hydraulic solver needs to be used to determine the wet-bulb temperatures from a simulation [46], [47], [51].

Three simulation packages are readily used in the reviewed literature, namely Vuma3D,[30] Process Toolbox[31] and Ventsim.[32] Each simulation package incorporates thermal-hydraulic solvers and is widely used in the evaluation of mine ventilation networks. Simulation models can also be built on the mine's drawing exchange format (DXF) layouts. The mine draws DXF files to map the current haulage and stoping developments and plan future developments. Thus, the mine's DXF files provide an accurate replication of the underground haulage sections and of future developments. Importing the mine's DXF files into a 3D simulation software package allows for fast and accurate 3D replications of the mine's ventilation network [45]. An example 3D network Ventsim simulation is shown in Figure 2-8. This figure illustrates the complexity and accuracy that these simulation models can achieve when built on the mine's DXF files and their ability to model mining ventilation networks in their entirety. The colour gradient of the image indicates changing

[30] Vuma 3D. (n.d.). *Vuma-network*. Retrieved July 6, 2023, from https://www.vuma3d.com/vuma-network/

[31] 3D mine ventilation simulation software

[32] Ventsim. (n.d.). *Ventsim 3D Mine Ventilation Simulation Software*. Retrieved July 6, 2023, from https://ventsim.com/

depths in the mine. However, these colour scales can be changed to represent ambient air temperatures and average air velocities in their respective regions of the mine.

Figure 2-8: Ventsim simulation package – 3D network example [59]

2.2.7 Step 7: Construct and calibrate model

Once a simulation package has been selected, a simulation model is constructed using the verified benchmarked data acquired in Section 2.2.3. A skeleton ventilation model should be constructed using the default component parameters. A ventilation simulation model is typically built with tunnel and node components, as illustrated in Figure 2-9.

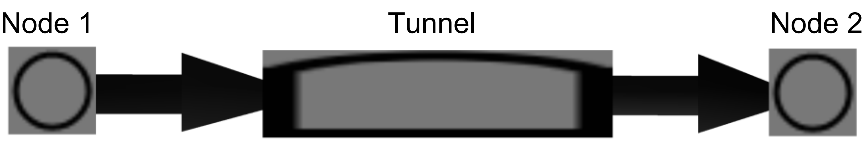

Figure 2-9: Process Toolbox tunnel and node pair[33]

Nodes provide simulation outputs relating to ambient air conditions such as temperature, relative humidity and pressure. Tunnels require dimensioning and provide airflow outputs such as velocity, mass flow and pressure drop over the specified length. The pressure differential is dependent on the tunnels' specified friction coefficient, which differs depending on the tunnels' lining types. Thus, the pressure output of Node 2 in Figure 2-9 is equal to that of Node 1 minus the pressure drop over the tunnel. Air boundaries are important components in ventilation

[33] Illustration by author.

simulations as they supply or absorb/take air to or from the system, acting as a source or sink of air with unlimited capacity.

The intake air way boundary acts as a source of ambient ventilation air at specified conditions, and the air boundary at the reject acts as a sink of air for the system. The pressure differential between these two points allows for flow to be initiated in the simulation, thus these air boundaries parameters are critical in the calibration of simulation models.

The simulation components (such as nodes, tunnels and boundaries) should be sized according to the benchmarked stope dimensions and constructed to replicate the benchmarked stope environment as illustrated in Figure 2-10.

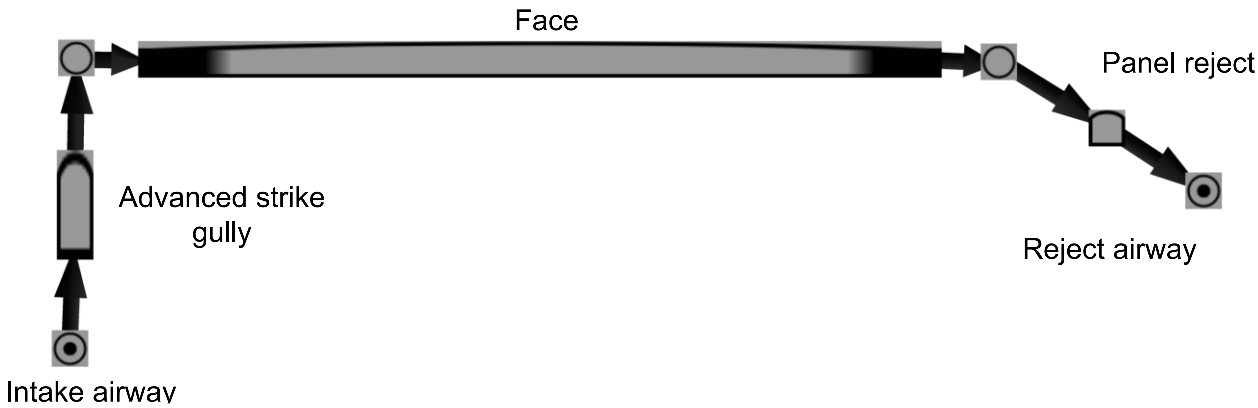

Figure 2-10: Process Toolbox replicated basic stope[34]

In Figure 2-10, the inlet airway is represented by an air boundary, indicating a source of inlet air at specified conditions. A tunnel connects the intake airway to the face of the stope through a node. From the face, the air flows to the panel reject and towards the reject airway. Thereafter, the reject airway is connected to another air boundary.

The initial parameters of the components should be adjusted iteratively to calibrate the simulation model with the ambient conditions of the benchmarked stope environment. The calibration and verification can be done as follows for the individual parameters:

Dry-bulb temperature [°C]

For tunnel sections, the heat transfer coefficients and virgin rock temperature are adjusted to obtain the correct dry-bulb temperature gain per section in the model [45]. These parameters adjust the amount of heat added to the air by each component.

[34] Illustration by author.

Wet-bulb temperature [°C]

For tunnel sections, the wet area fraction or moisture content is adjusted to obtain the correct wet-bub temperature. This effectively changes the humidity ratio and calibrates the amount of moisture that each component adds to the air [45].

Barometric pressure [kPa] and air mass flow [kg/s]

The barometric pressure of the stope environment influences the airflow through the stope environment. The benchmarked barometric air pressure value should be assigned to the inlet component of the model stope environment. To obtain the correct airflow through the stope, the airflow resistance of the tunnel components should be adjusted [45]. A lower resistance (lower pressure difference) results in a higher flow, whereas a higher resistance (higher pressure difference) results in a lower flow.

Model verification

The simulation should be calibrated to within 5% of the actual verified values [47], [59]. However, according to Nel [51] and Clarke [60], an error of 10% or lower is acceptable in the mining industry for flow measurements. The accuracy of the simulation model is to be determined using the mean absolute error (MAE) method.

Equation 2-5: Mean absolute error [45]

$$Error_{\%} = \frac{1}{k}\sum_{k=1}^{K}\left|\frac{A_k - S_k}{A_k}\right|(100\%)$$

Where

$Error_{\%}$	=	Percentage error	%
K	=	Total number of data points	−
k	=	Total number of data points	−
A_k	=	Actual data point	−
S_k	=	Simulated data point	−

Once the simulation model is calibrated to within 5% of the verified benchmarked system, the simulation model is considered validated as it accurately replicates the environmental conditions of a real-world environment within an acceptable margin.

2.2.8 Step 8: Simulate operational change simulation

From the calibrated simulation model, the varying operational changes identified in Section 2.2.1 and heat load changes identified in Section 2.2.5 are implemented into the calibrated simulation to create an operational change simulation. Thereafter, the operational change simulation model is simulated and the results evaluated against the identified KPIs boundaries identified in Section 2.2.4. This evaluation determines if the implemented operational change still adheres to the original simulation boundaries or if amendments need to be made to the operational change simulation.

2.2.9 Step 9: Evaluate results (final KPI validation)

Finally, the results for each operational change simulation are evaluated against one another and the calibrated simulation. The results of the simulations are tabulated to compare the relative change between the operational changes and the benchmarked system. This evaluation determines the nett effect of each operational change and evaluates each system's operational efficiency according to the identified KPIs. From this evaluation, the optimum operational change is either identified or the nett effect of the operational change is quantified.

2.3 Method verification

The stope heat load method developed, as detailed in Sections 2.2.1–2.2.9, is discussed in the following section with the intent of explaining how the method aids in achieving each study objective. Referring to the first study objective, the stope environment needs to be defined in order to simulate its heat load characteristics.

Steps 1–3 of the method define the stope environment. These steps ensure that the stope environment is defined, that the stopes parameters are benchmarked accurately and that they are verified. These steps are illustrated in Figure 2-11.

Step 4 begins to classify Study Objective 1.1. In order to quantify the heat added/removed from the stope environment, the KPIs of the stope environment that characterise the environmental conditions and its heat need to be selected.

Step 5 quantifies the heat addition or removal of the identified operational change. The boundary of concern around the operational environment is identified first to determine the energy forms entering and exiting the boundary perimeter at any time.

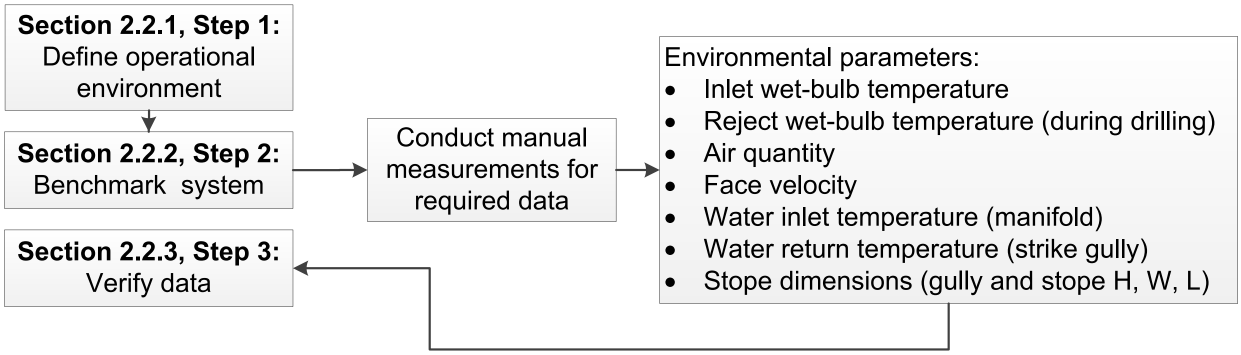

Figure 2-11: Sections 2.2.1–2.2.3 of the method[35]

Thereafter, the heat sinks and heat sources in the stope environment are determined to quantify the amount of energy added or removed by various mechanisms. Finally, a balance of the energy forms is done to quantify the nett heat added or removed from the stope environment. This step finalises Study Objective 1.1. Steps 5 and 6 are illustrated in Figure 2-12.

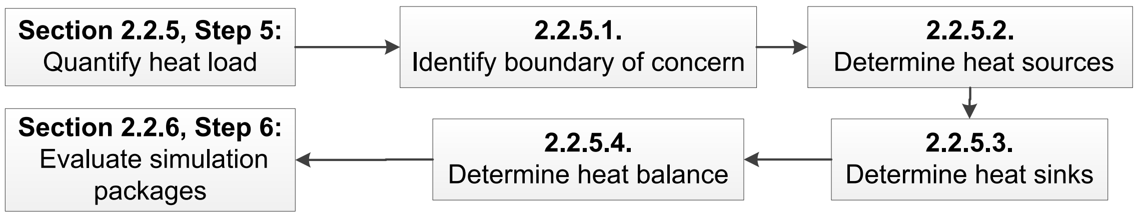

Figure 2-12: Sections 2.2.5 and 2.2.6 of the method

Step 6 evaluates available simulation software that can determine the required outcomes. A thermal-hydraulic solver is needed to determine the heat load. Three programs are used regularly for ventilation simulations.

Step 7 constructs and calibrates the simulation model to within an acceptable margin for the mining industry, thus validating the model against the benchmarked real-world stope environment. From this comparison, Study Objective 1.2 is achieved by comparing and validating the simulation results.

Steps 8 and 9 allow for the prediction of thermal changes when micro-hydropower technologies are introduced into the stope. This is done by introducing hydropower technology into the simulation as an operational change and adding the quantified heat addition or removal of heat

[35] Adapted from [46], [47].

for the operational change in Step 5. The effects of the nett heat are thus determined from the simulation. Therefore, achieving Study Objective 2.1.

Finally, the calibrated simulation is adapted to include multiple stopes daisy-chained in series to evaluate a theoretical mining raise line. This allows for the environmental effects for more than one stope to be analysed. The results of this simulation for both the benchmarked and hydropower systems may identify possible operational constraints due to the changing environmental conditions. This analysis achieves the final Study Objective 2.2.

Table 2-1 summarises the method steps in which each study objective has been successfully addressed.

Table 2-1: Study objectives addressed in method steps

	Objective 1.1	**Objective 1.2**	**Objective 2.1**	**Objective 2.2**
Step 1	✓			
Step 2	✓			
Step 3	✓			
Step 4	✓			
Step 5	✓			
Step 6		✓		
Step 7		✓		
Step 8			✓	
Step 9				✓

2.4 Method summary

All the above-mentioned steps are combined into a flow diagram as illustrated in Figure 2-13.

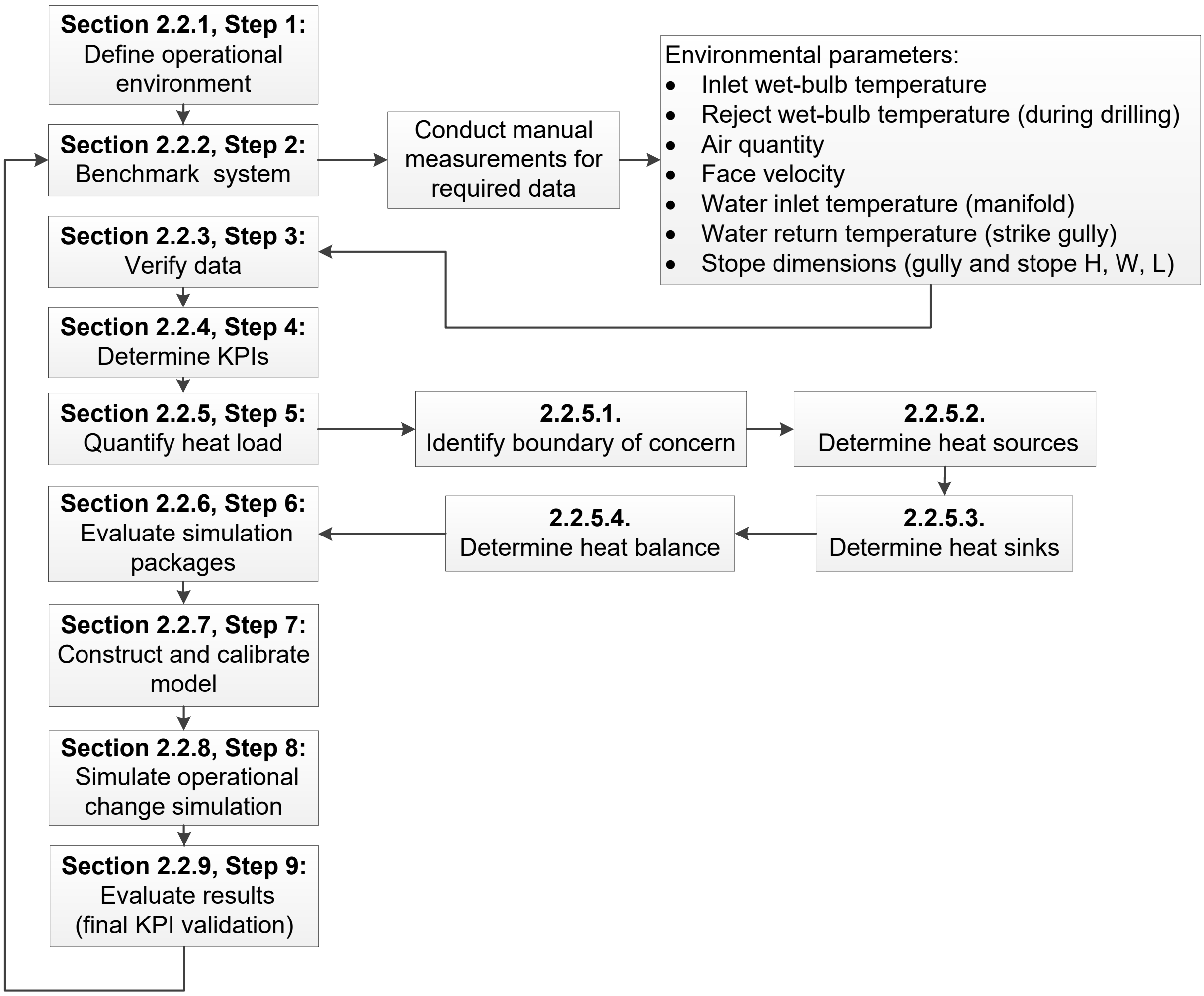

Figure 2-13: Proposed stope heat load method flow diagram

2.5 Conclusion

A method was developed from the literature to address the study objective needs. The method was detailed in the method development in Section 2.2. Once the method was developed, a method flow diagram was created. Each step of the flow diagram was elaborated on with the aim of indicating how the developed method will enable the identified study objectives achievement to be achieved.

CHAPTER 3 – IMPLEMENTING THE METHOD: RESULTS AND DISCUSSION

3.1 Preamble

In this chapter, the developed stope heat load method was applied to a case study mine. The case study mine is a platinum mine located in the North-West province of South Africa. A conventional pneumatic stope environment was converted to a micro-hydropowered stope. The conversion was done as part of a proof-of-concept trial for micro-hydropower technology on the mine with the goal of comparing the performance of a micro-hydropowered stope to a conventional stope. The trial was initiated due to the reducing compressed-air pressures in their compressed-air reticulation network. As discussed in Section 1.3, inadequate compressed-air pressures reduce the penetration rates of pneumatic drills and thus reduce the productivity of crews.

3.2 Application of method

The method depicted in Figure 2-13 is applied in this section and a detailed explanation is given for each step. An overview of the conventional pneumatic stope layout to be benchmarked and converted to hydropower in this case study was shown in Figure 1-4.

3.2.1 Step 1: Define operational environment

The operational environment of this case study was a platinum, conventionally powered, compressed-air stope environment. The stope had to be converted/retrofitted with a micro-hydropower system. Thus, the operational change for this case study was the addition of hydropower drills and removal of compressed-air drills from the stope environment.

The hydropower drills were supplied by a single 55 kW power pack situated in the raise line near the active panel. The stope set-up remained the same as the conventional stope regarding the number of drills and the hydropower panel layout, as depicted in Figure 1-12. Thus, the hydropowered stope environment had a higher instantaneous water consumption and an increase in the electrical load per drill as outlined in Table 1-2 when comparing the alternative drilling technologies.

3.2.2 Step 2: Benchmark system

Once the operational environment has been determined, it needs to be benchmarked. However, benchmarking entails the full characterisation of the stope's environmental conditions and any factors that influence the environment.

Firstly, the stope's physical dimensions were recorded for the stope environment to be replicated accurately in the simulation model. It was seen that the airflow distribution was not uniform in the stope. Thus, the ventilation air velocity along the face of the panel was recorded. This was the region where rock drill operators operated and was the region where the localised drill effects would be experienced.

An illustration of the stope airflow distribution with the dimensions of the operational environment is provided in Figure 3-1. The dashed brown line illustrates a brattice, which is a fireproof sheet that is fixed to the hanging or side walls in a stope environment. It is a ventilation control device for providing temporary airflow guidance in stope environments [45].

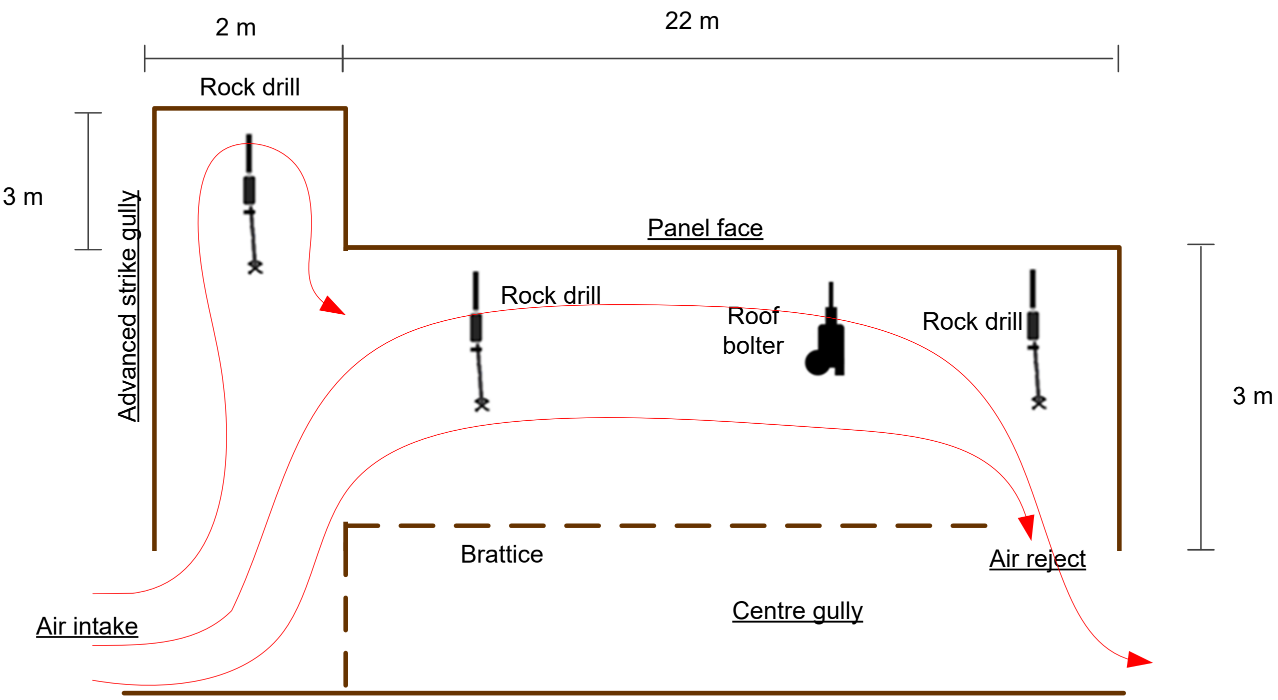

Figure 3-1: Stope airflow distribution[36]

[36] Illustration by author.

Figure 3-1 illustrates the flow distribution and non-uniform nature of the flow. Airflow distribution affects the construction of the simulation model in order to replicate the real-world stope as best as possible. The basic stope model given in Figure 2-10 assumes a uniform airflow distribution.

Once the physical dimensions of the stope were noted, environmental parameters for the conventional compressed-air stope were measured to define the stope environment fully. Once the stope environment had been converted, the micro-hydropowered stope environment was also benchmarked according to the same procedures as the conventional panel.

Manual measurements were taken following the methods stated in Section 2.2.2 as the accuracy of these measurements are critical. The benchmarked environmental parameters for the compressed-air and micro-hydropowered stope environments are tabulated in Table 3-1.

Table 3-1: Environmental parameters

Parameter	Unit	Compressed air	Hydropower
Inlet wet-bulb	°C	24.0	17.8
Inlet dry-bulb	°C	27.5	26.0
Reject wet-bulb (during drilling)	°C	27.0	22.0
Reject dry-bulb (during drilling)	°C	27.5	27.0
Localised wet-bulb at face (before drilling)	°C	26.6	25.4
Localised dry-bulb at face (before drilling)	°C	27.0	29.1
Localised wet-bulb at face (during drilling)	°C	25.5	27.6
Localised dry-bulb at face (during drilling)	°C	25.5	28.7
Intake air quantity	kg/s	0.6	0.6
Face air velocity	m/s	0.4	0.4
Water inlet temperature (manifold)	°C	23.5	21.6
Reject water temperature (drill)	°C	25.0	25.4
Water return temperature (strike gully pump)	°C	26.9	26.8
Stope dimensions (H, W, L)	m	1.2, 3, 22	1.2, 3, 22
Gully dimensions (H, W, L)	m	2.5, 3, 2	2.5, 3, 2
Drill water consumption	L/s	0.2	0.7
Power pack max water consumption	L/s	NA	2.9

Certain measurements are taken before and during drilling operations to determine the influence that the drilling operations have on the environmental parameters within the panel. The location of the measurements within the respective panels can be seen in Figure 2-7 and Figure 3-5.

3.2.3 Step 3: Verify data

As described in the method in Chapter 2, the values were measured iteratively until the percentage error between the recorded values were within 5% of one another. Figure 3-2 illustrates the measured intake wet-bulb temperatures that were measured iteratively. As can been seen in the figure, the recorded measurements were within the 5% upper and lower bounds, and the average of these measurements was taken as the inlet wet-bulb temperature. The same process was followed for each of the parameters given in Table 3-1.

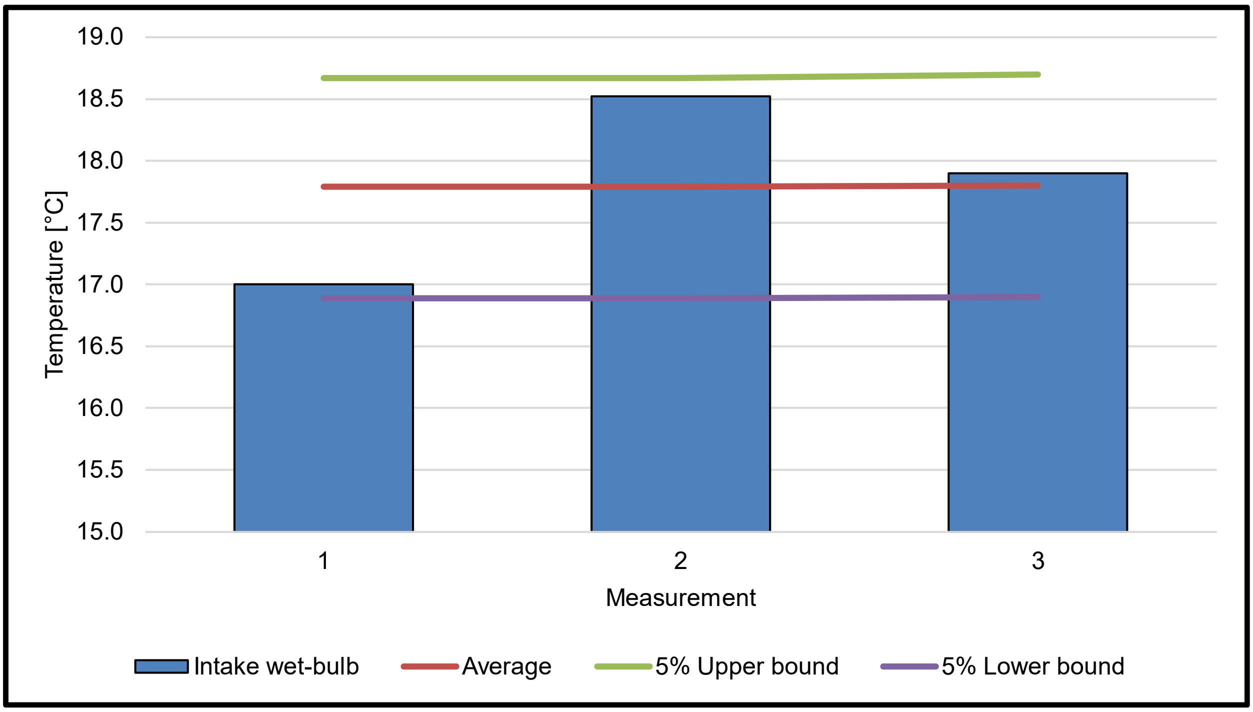

Figure 3-2: Measured intake wet-bulb temperatures

3.2.4 Step 4: Determine KPIs

The conversion of the conventional stope environment to a micro-hydropowered stope introduces heat into the stope environment through the power pack and removes the localised cooling effect of the compressed-air drills. Thus, the stope's environmental conditions reflect the heat load change through an increase or decrease in the reject ambient air conditions. Therefore, the KPIs for this study are the stope's reject wet-bulb and dry-bulb temperatures during drilling operations and the heat added or removed from the stope.

The KPI boundaries were the thermal stress exposure temperature limits as defined in the *Mine Health and Safety Act 29 of 1996* [41]. Since any workplace exceeding these limits is deemed unsafe, these limits acted as boundaries/constraints in the simulation. The identified boundaries for the simulation concerning the identified KPIs are given in Table 3-2.

Table 3-2: Simulation boundaries

Parameter	Unit	Value
Reject dry-bulb (during drilling)	°C	37.0
Reject wet-bulb (during drilling)	°C	32.5

3.2.5 Step 5: Quantify heat load

The heat load over the stope environment is an important analysis parameter for the simulation as it determines whether heat is added or removed from the stope. Firstly, the boundary of concern needs to be defined, whereafter the heat sources, heats sinks, and heat balance should be determined following the steps outlined in Figure 3-3.

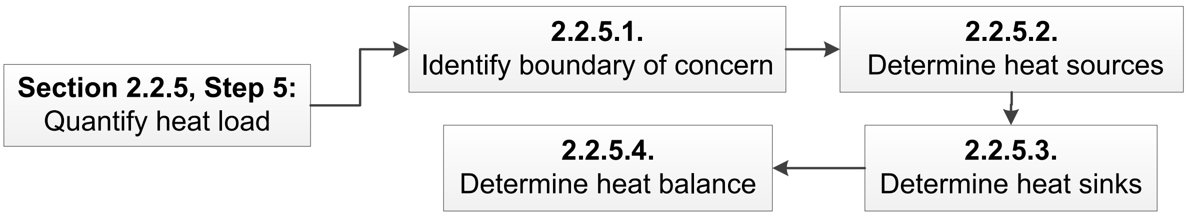

Figure 3-3: Heat load quantification steps

3.2.5.1 Identify boundary of concern

A holistic energy balance was evaluated over the stope environment to ensure all of the energy forms entering and exiting the boundary of concern were accounted for. For a conventional stope environment, these include service water, compressed air and ventilation air. The boundary of concern for a conventional stope environment is depicted in Figure 3-4.

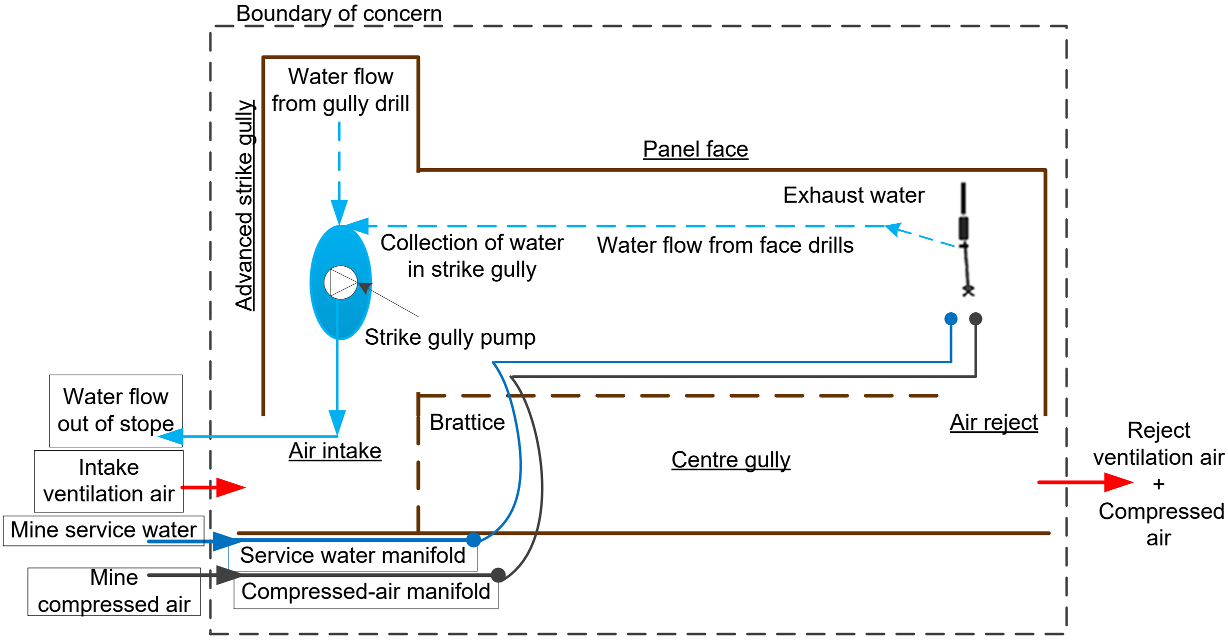

Figure 3-4: Compressed-air stope boundary of concern[37]

The red arrows entering and exiting the boundary of concern represent the ventilation air, similarly, the blue arrows represent the service water. Note that the compressed air entering the stope environment with a black arrow exits the boundary of concern along with the ventilation air as it is exhausted to the atmosphere during operation. As discussed in the selection of KPIs in Section 3.2.4, the reject ambient air conditions of the stope environment were used to determine the heat load effect over the stope environment.

Therefore, due to the reject ambient air conditions being inclusive of the exhausted compressed air from the drills, the heat load effect of the compressed air was included in the evaluation of the reject ambient air conditions. The analysis of compressed-air parameters and the determination of their energy input were negated for the purpose of this study. This is because the purpose of the study objectives was to determine the heat load characteristics of a stope environment, done through the reject ambient air conditions, and to predict the thermal changes when implementing micro-hydropower technologies, and not to predict changes when compressed-air parameters are altered.

For the micro-hydropower environment, the boundary of concern included a hydropower power pack that required an electrical supply cable (yellow) and did not have any compressed-air supply

[37] Illustration by author.

from the mine. A simplified boundary of concern for a micro-hydropower stope is depicted in Figure 3-5.

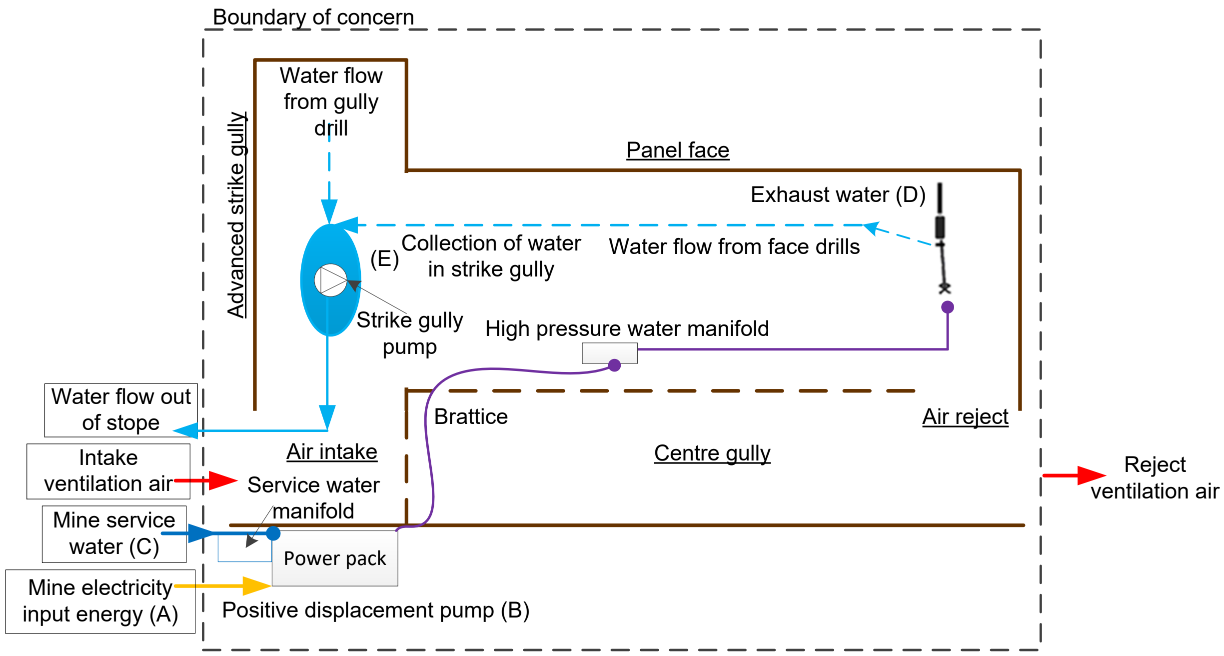

Figure 3-5: Boundary of concern over the hydropowered stope [38]

Figure 3-5 shows that the evaluation of the boundary starts at Point A with the amount of electrical energy delivered to the system by the electric motor. The motor drives the pump and the energy is transferred to the pump and Point B after accounting for the efficiency of the motor. Thereafter, the service water enters the pump at Point C and the high-pressure water flows towards Point D at the drill. The water is used to drive the drill and cool the drill collar, drill bit and flush the hole. The water is dumped onto the foot wall and is collected in the strike gully E. From here, the water is dewatered out of the boundary of concern.

3.2.5.2 Determine heat sources

Consider the identified boundary of concerns for the compressed air and micro-hydropowered stope environments. The 55 kW power pack adds potential energy into the water system in the hydropower stope environment. To account for the potential energy/heat added to the water by the power pack, Points C and D of Figure 3-5 are important. By using the maximum water flow rate for each drill in the stope environment, the nett heat added to the water by the power pack was determined by applying the heat duty formula given in Equation 2-1. The amount of heat

[38] Illustration by author.

added to the water over the drills in both environments was determined for a comparison between the two technologies as tabulated in Table 3-3.

Table 3-3: Water heat source summary

Point	Parameter	Unit	Compressed air	Hydropower	Difference (Hydropower − Compressed air)
C	Manifold inlet water temperature	°C	23.5	21.6	−1.9
D	Reject water temperature at drill	°C	25.0	25.4	0.4
	Delta (C − D)	°C	1.5	3.8	2.3
	Maximum flow rate through running drills	L/s	1.0	2.9	1.9
	Heat	kW	6.3	46.1	39.8

The heat gain in the service water from the compressed-air drills [Delta (C − D)] is attributed to the frictional heat of the drilling itself as the service water is used to cool the drill bit and drill and flush the hole. This heat gain is applicable to the hydropower drills as well; however, the hydropower system increased the Delta (C – D) temperature by 2.3 °C, resulting in an additional 39.8 kW of heat being added into the service water along with the higher water flow rates.

3.2.5.3 Determine heat sinks

From the boundary of concern depicted in Figure 3-5, mine service water and ventilation air are seen to enter and exit the boundary. Both water and air act as a heat sink in the environment by removing heat from the stope environment. Thus, the heat added or removed from both mediums had to be determined.

To determine the amount of heat removed by the water over the stope, Points C and E are important in Figure 3-5. Both stope environments had very good return water controls in place by installing a water pump in the strike gully. This pump removes the pooling wastewater from the drills and limits the contact time between the intake air and return water.

By using the maximum water flow rate for each drill in the stope environment, the nett heat removed from the stope environment by the water was determined by applying the heat duty formula given in Equation 2-1. The calculated heat sinks are tabulated in Table 3-4.

Table 3-4: Water heat sink summary

Point	Parameter	Unit	Compressed air	Hydropower	Difference (Hydropower – Compressed air)
C	Manifold inlet water temperature	°C	23.5	21.6	−1.9
E	Water temperature in strike gully	°C	26.9	26.8	−0.1
	Delta (C − E)	°C	3.4	5.2	1.8
	Maximum flow rate through running drills	L/s	1.0	2.9	1.9
	Heat removed	kW	14.2	63.1	48.9

From Table 3-4, both stope environments removed heat from the stope environment and thus had sufficient water controls. However, the hydropower stope environment removed 48.9 kW more heat from the stope environment, which was largely due to the greater temperature delta between the service water entering the stope and the water exiting the stope at the strike gully. This indicates that more energy was added to or picked up by the water in the hydropowered stope environment. The amount of heat added to the water by the drills was determined in Section 3.2.5.2.

For the ventilation air, the localised heat effect of both the compressed-air and hydropower drills was determined by measuring the ambient conditions of the face area before and during drilling as depicted in Figure 2-7. The measured temperatures of the two regions for both the compressed-air and hydropowered stope environments are illustrated in Figure 3-6.

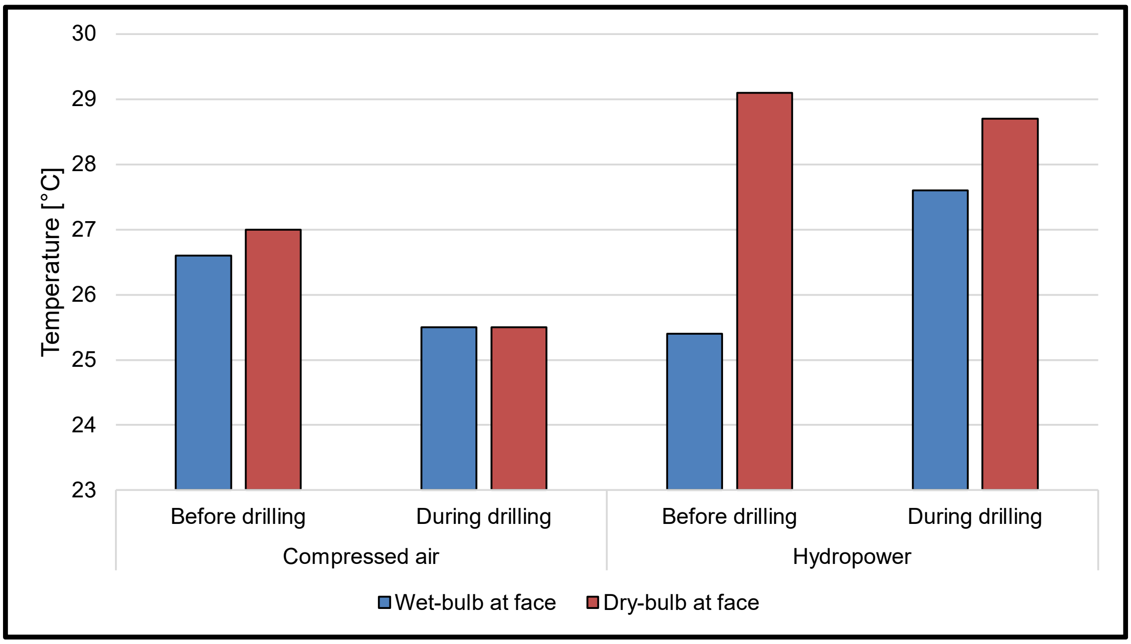

Figure 3-6: Measured localised face temperatures

From Figure 3-6 illustrates the cooling effect of the compressed-air drills on the localised environment by a reduction in the dry-bulb and wet-bulb temperatures during drilling. Whereas a heating effect was seen with the hydropower drills as the wet-bulb temperature increased. The nett heat effect from the different drill types was determined by evaluating the enthalpy difference of the localised air before and during drilling using Equation 2-3. This was evaluated and is tabulated in Table 3-5.

Table 3-5: Ventilation air heat sink summary

Parameter	Unit	Compressed air	Hydropower
Enthalpy (before drilling)	kJ/kg	84.7	79.0
Enthalpy (during drilling)	kJ/kg	79.6	89.1
Delta enthalpy	kJ/kg	−5.1	10.2
Air mass flow	kg/s	0.6	0.6
Heat	kW	−2.8	6.0

From the localised conditions around the face area and drills, the compressed-air drills cooled the localised environment by reducing the enthalpy of the air after the drills and thus introduced 2.8 kW of cooling over the stope. However, the hydropowered drills increased the enthalpy of the ventilation air and thus added 6.0 kW of heat over the stope. A heat balance is done in the following section to determine the overall effect of the hydropower heat addition.

3.2.5.4 Determine heat balance

The geothermal heat source in the stope environment was determined through a heat balance of the identified heat sources and heat sinks. For the water system, the geothermal heat was determined by calculating the heat pick-up between Points D and E of Figure 3-5 or by performing a heat balance between Points C to D and Points C to E.

In the compressed-air stope environment, 14.2 kW of heat was removed from the stope environment by the water, Points C to E, of which 6.3 kW was heat pick-up over the drills, Points C to D. Thus, 7.9 kW of heat was added to the water by the stope environment through heat transfer from the rock, which was geothermal heat gain. The compressed-air heat balance is depicted in Figure 3-7, with blue bars indicating heat pick-up and orange bar indicating heat removal from the water system. For the ventilation air network, green indicates a reduction of heat from the air network and red an increase or addition.

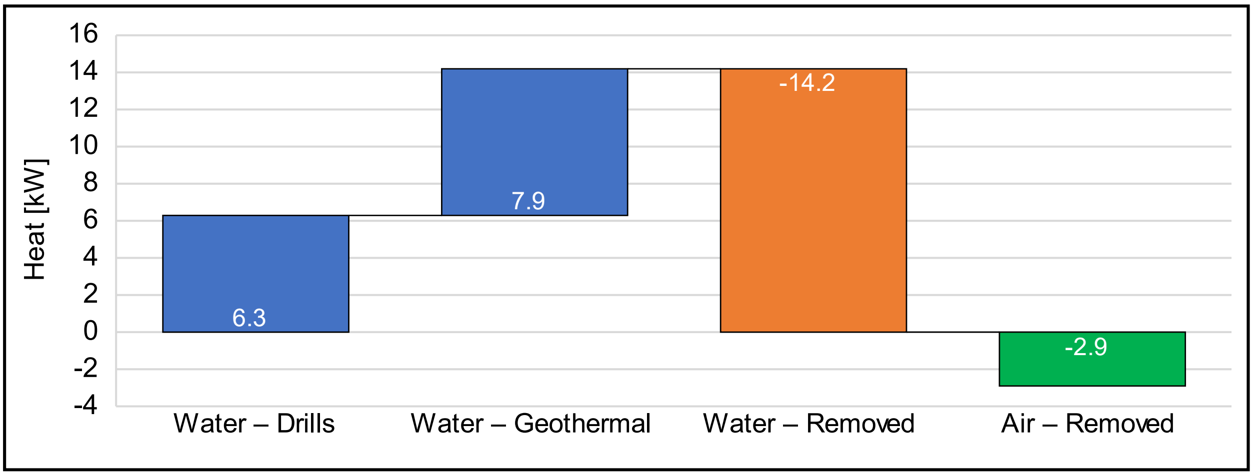

Figure 3-7: Compressed-air heat balance

Following the same steps for the hydropower stope in Figure 3-5, the geothermal heat source was determined to be 17 kW. This increase in geothermal heat transfer for the hydropower stope was attributed to the increase in water flow rate as the compressed-air and hydropower drill water temperatures and gully temperatures were very similar. The hydropower heat balance is depicted in Figure 3-8.

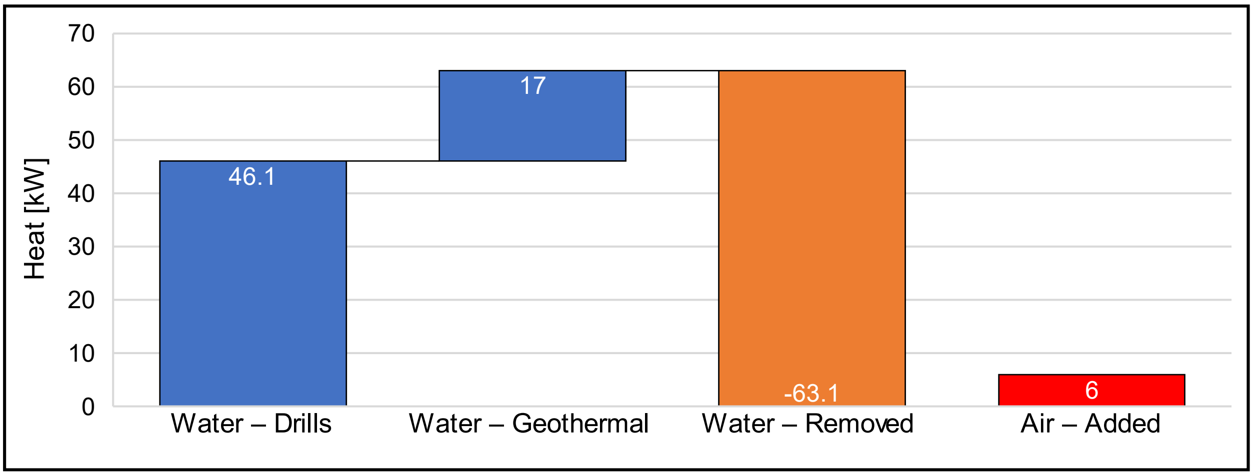

Figure 3-8: Hydropower heat balance

The evaluation of the stope heat load aimed to determine to what extent heat was transferred to the water between Point A/C and Point D and how much of that heat was liberated into the air. In the hydropower environment, the results yielded that approximately 46.1 kW of the total input energy (55 kW) could be measured at Point D. This means that 83.9% of the energy transferred to the water ended up as internal heat gain. Additionally, of the 46.1 kW of heat, 6.0 kW was liberated to the air. This means that of the total input energy (55 kW), 40.1 kW could effectively be removed through good water controls in the stope. Thus, of the total 63.1 kW heat removed by the water from Table 3-4, 40.1 kW was attributed to the power pack.

Regarding the compressed-air and hydropower stope environments, the hydropower stope removed more heat through the water system, yet an increase in the reject ambient air conditions was recorded. A comparison of the heat balance of each environment showed that the hydropower stope removed 48.9 kW more heat than the compressed-air stope. However, of the 48.9 kW, 39.8 kW was additionally added to the stope environment by the introduction of the hydropower power pack. The hydropower stope also saw an increase in the geothermal heat pick-up, which could be attributed to the increased water flow rate. This increase in geothermal heat of 9.1 kW made up for the heat imbalance between 48.9 kW and 39.8 kW. This step concluded the quantification of the heat added/removed from the stope environment (Objective 1.1).

3.2.6 Step 6: Evaluate simulation packages

A thermal-hydraulic simulation software was needed for this application as the heat load over the stope environment would be determined from the simulation's ability to determine ambient wet-bulb conditions. Process Toolbox was used to simulate the heat load characteristics of the stope environment as it can solve ventilation and mine cooling systems in a single integrated model [46]. This ability was beneficial due to the complex nature of the stope environment with multiple heat sources and sinks.

3.2.7 Step 7: Construct and calibrate model

From the compressed-air case study stope environment, the dimensions of the localised environment were measured and replicated in a simulation model constructed in Process Toolbox. The non-uniform airflow distribution noted in Figure 3-1 of the benchmarking step was implemented into the simulation model by separating the stope into panel face and stope back regions. The stope layout can be seen in Figure 3-9 with the ventilation flow directions indicated by red arrows. The location of the handheld rock drills is also depicted in the panel face area of the stope.

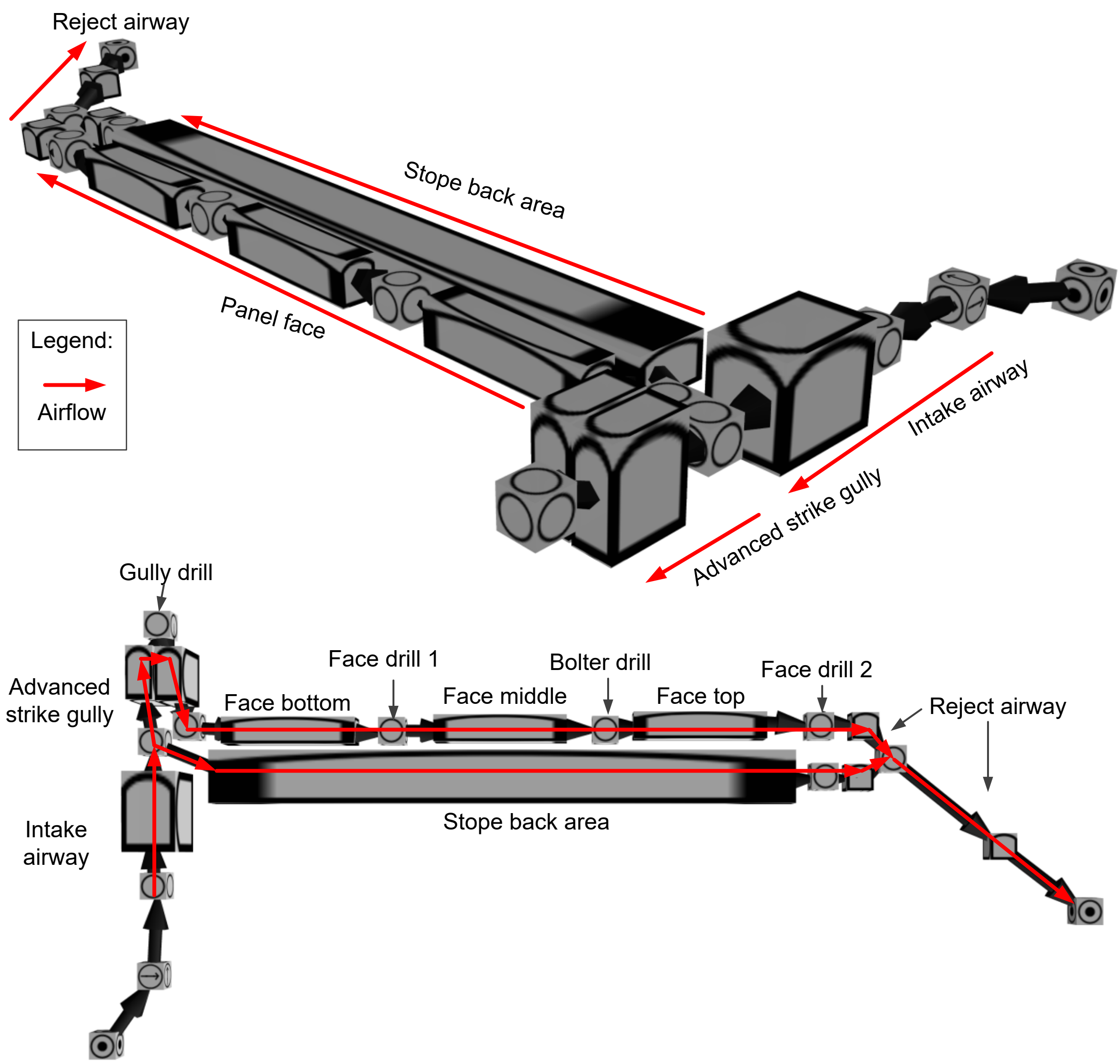

Figure 3-9: Simulated stope environment

The data obtained from benchmarking the system in Section 3.2.2 was programmed into the simulation model. Thereafter, the baseline compressed-air model was calibrated using an iterative approach by changing the characteristics of the model environment to match those of the actual environment. The calibration included replicating the face velocity measured in the panel face region of the stope environment.

For the purpose of this study, it was assumed that the airflow for the face region passed through the gully area first and that the airflow from the intake airway could either flow towards the gully or short-circuit through the stope back region before combining again at the reject airway. The reject ambient air conditions were baselined and the calibration evaluated at the combination airflow point of the reject airway. The calibrated baseline results are compared with the actual measurements in Table 3-6.

Table 3-6: Baseline simulated results

Parameter	Unit	Actual	Baseline simulation
Reject dry-bulb during drilling	°C	27.5	27.9
Reject wet-bulb during drilling	°C	27.0	27.1

Using the MAE method given in Equation 2-5, the error percentage of the simulation was determined and tabulated in Table 3-7.

Table 3-7: Baseline simulation MAE

Parameter	Unit	MAE
Reject dry-bulb during drilling	%	1.5
Reject wet-bulb during drilling	%	0.4

From the MAE error percentages of Table 3-7, it was concluded that the second study objective was achieved by creating and validating a simulation model to a real-world stope environment within 5% accuracy (Objective 1.2).

To achieve Study Objective 2.2, the baseline simulation model was expanded by daisy-chaining multiple stopes in series to replicate a compressed-air raise line in an underground mine, as shown in Figure 3-10. This model assumed that all of the reject stope ventilation air of a stope was recycled for the inlet ventilation air of the following stope in series, simplifying the raise line ventilation network.

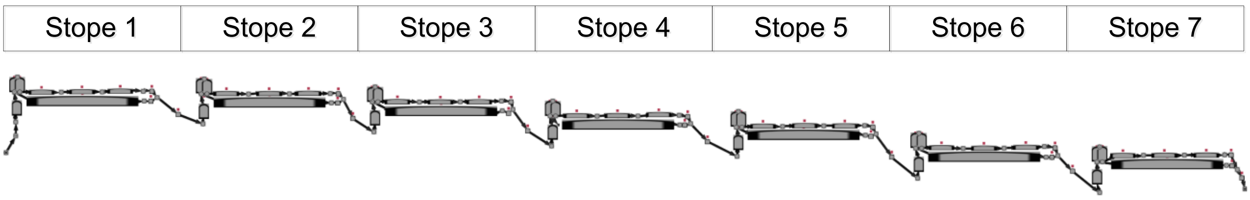

Figure 3-10: Raise line simulation model view

The simulation was run to determine the ventilation air conditions throughout the raise line for the baseline compressed-air model. The simulated raise line wet-bulb temperature profile for the stopes in series is depicted in Figure 3-11.

Figure 3-11: Compressed-air raise line wet-bulb temperature profile

It is clear that the temperatures in the stopes increased along the raise line. The temperatures are illustrated by a colour gradient (blue, green, yellow and red) with blue being the coldest and red indicating the hottest simulated wet-bulb temperatures. The yellow colour gradient indicates the transition to and from the wet-bulb temperature boundary of 32.5 °C. The simulated reject stope temperatures of Figure 3-11 are graphed in Figure 3-12.

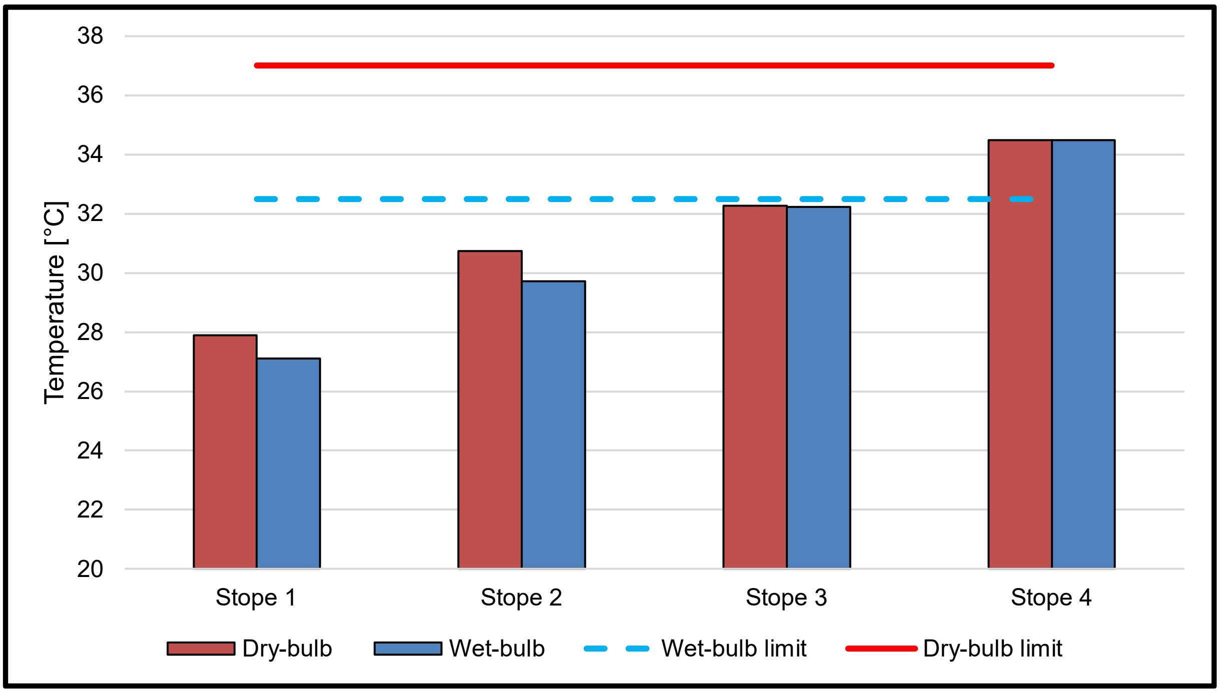

Figure 3-12: Simulated compressed-air stope reject temperatures

The first simulated compressed-air stope had reject wet- and dry-bulb temperatures of 27.1 °C and 27.9 °C, respectively. Figure 3-12 shows that the third stope in the series had a reject wet-bulb temperature nearing the KPI boundary of 32.5 °C, whereas the fourth stope's reject wet-bulb temperature exceeded the legal temperature limits as outlined in Section 3.2.4.

3.2.8 Step 8: Simulate operational change

The identified operational change for this case study is the conversion of a conventional compressed-air stope environment to a micro-hydropower stope environment. Thus, the hydropower drills will add heat to the environment and the removal of pneumatic drills from the stope environment will remove localised cooling. The heat load characteristics for the baseline compressed-air stope model of Section 3.2.7 were changed to that of the hydropowered stope, as given in Table 3-5. The raise line model was simulated with the updated hydropower heat load. The simulated temperature profile for the raise line is depicted in Figure 3-13.

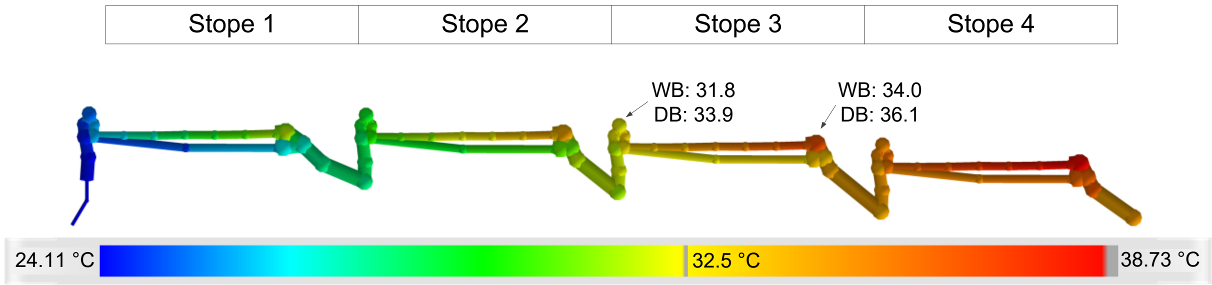

Figure 3-13: Hydropower raise line wet-bulb temperature profile

The simulated hydropower stope temperatures increased along the raise line similarly to those of the baseline compressed-air model. The same temperature colour gradient of the compressed-air environment was used to illustrate the relative difference between the two models. It is clear from Figure 3-13, however, that the hydropowered raise line reached the boundary wet-bulb temperature of 32.5 °C in the third stope as the reject wet-bulb temperature of the third stope was 34.0 °C. The stope's reject temperatures of the hydropowered raise line are depicted in Figure 3-14.

Figure 3-14 shows that the first simulated hydropowered stope had reject wet-bulb and dry-bulb temperatures of 27.7 °C and 30.0 °C, respectively. The wet-bulb temperature exceeded the legal temperature limits in the third stope as the reject wet-bulb temperature was above 32.5 °C. In the fourth stope, the dry-bulb temperature boundary was exceeded as the reject dry-bulb temperature was 38.9 °C. From these simulation results, the effect of additional heat on the environmental conditions in the stope environment was determined (Objective 2.1).

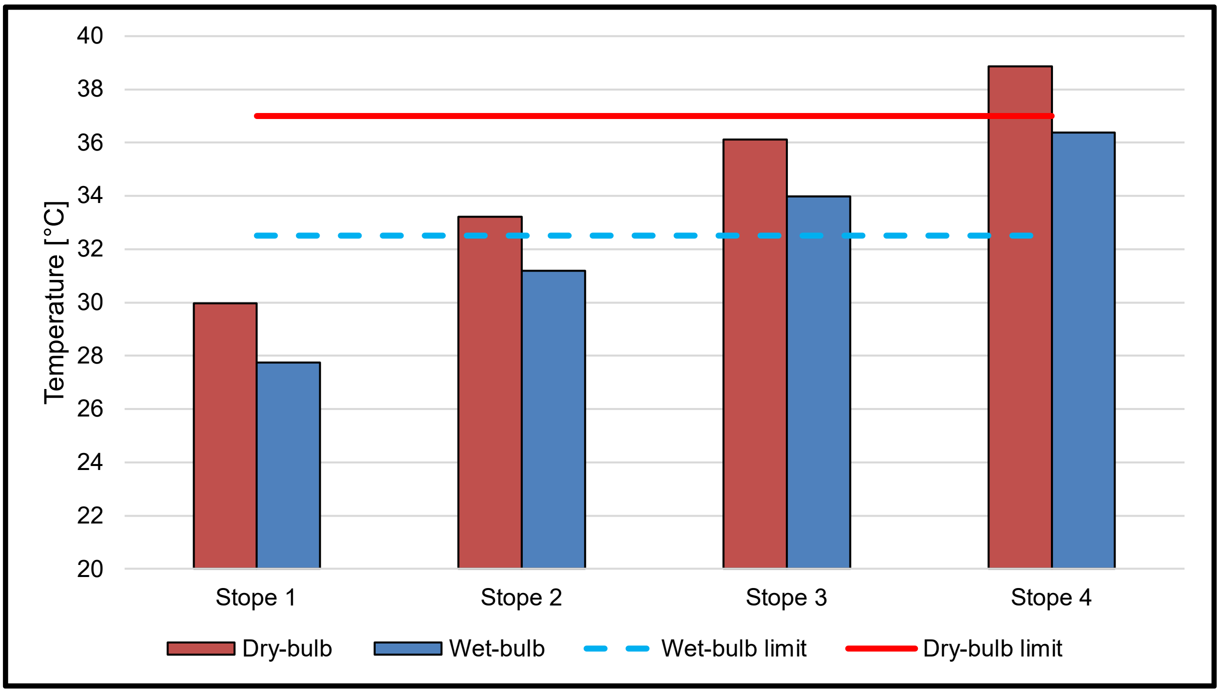

Figure 3-14: Simulated Hydropower stope reject temperatures

3.2.9 Step 9: Evaluate results (final KPI validation)

The simulated hydropower stope had higher reject temperatures than those of the baseline compressed-air stope. The comparative simulation results for the baseline and the hydropower operational change are shown in in Table 3-8.

Table 3-8: Comparative KPI results

Parameter	Unit	Baseline simulation	Hydropower	Delta T
Reject dry-bulb during drilling	°C	27.9	30.0	2.1
Reject wet-bulb during drilling	°C	27.1	27.7	0.6

From the simulation results it was concluded that the hydropower stope conversion added 0.6 °C to the reject wet-bulb temperature and 2.1 °C to the reject dry-bulb temperature. This temperature increase was also seen across the raise line as the third hydropowered reject stope wet-bulb temperature (34.0 °C) was 1.8 °C higher than that of the third compressed-air reject stope wet-bulb temperature (32.2 °C). The comparative reject compressed-air and hydropower stope wet-bulb temperatures are shown in Figure 3-15.

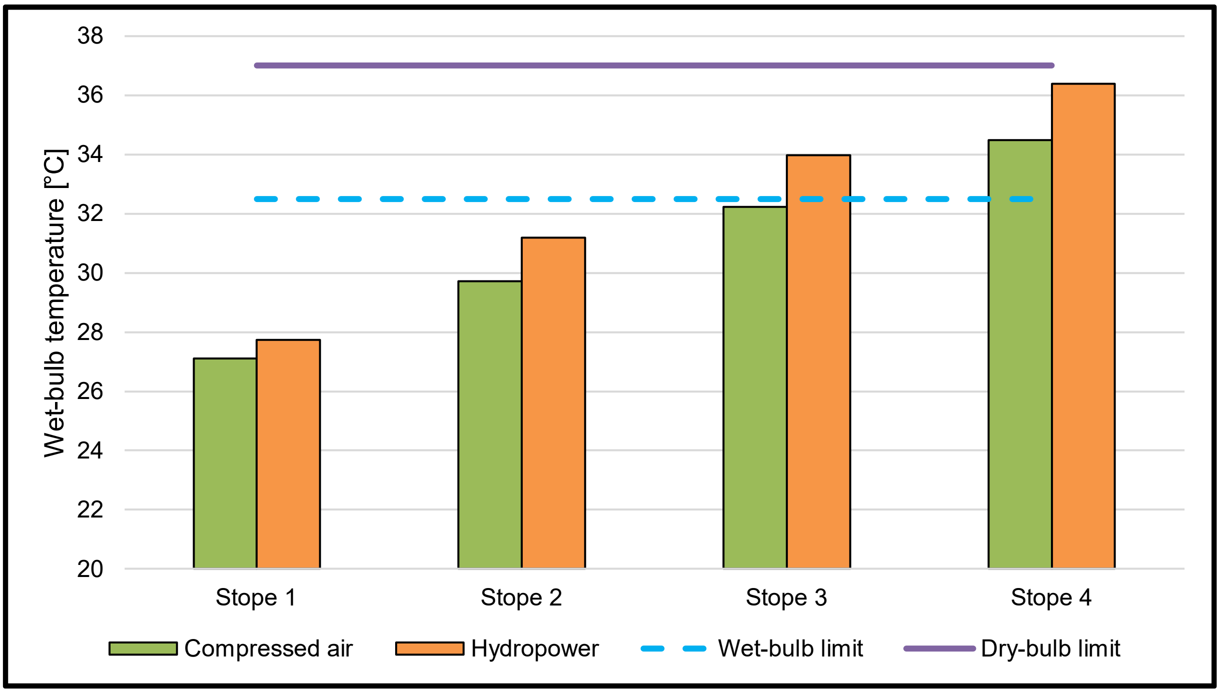

Figure 3-15: Simulated compressed-air and hydropower stope reject wet-bulb temperatures

It is clear from Figure 3-15 that the hydropower stope environments consistently had higher stope reject temperatures. As discussed in Section 1.4.4, an increase in the ambient temperature reduces worker production efficiency and increases the risk of heat injuries such as heat exhaustion, heat cramp and heatstroke.

Figure 1-13 showed that the estimated production efficiency of a labourer in the third compressed-air stope environment would be around 84%. Comparatively, a labourer's production efficiency in the third hydropowered stope environment would be 56%. The hydropowered stope environment would also be at a greater risk of heat injuries due to the increase in temperature.

Through the analysis of the simulation results of the compressed-air and hydropowered stope environments, the effect on the environmental conditions was determined for multiple converted stopes (Objective 2.2). Additionally, the effect of these changes on labourers in the stopes was discussed.

3.3 Validation of method

Following the application of the stope heat load method on the case study mine, *Objective 1.1: Quantify heat added/removed from the environment* was successfully achieved by applying Steps 1–5 of the method. The conventional compressed-air stope environment was seen to cool the localised ambient air conditions by adding 2.8 kW of cooling, whereas micro-hydropower was seen to add 6 kW of heat to the air. The heat balance of the stope environments showed that although the hydropower stope was seen to remove more heat relative to the compressed-air stope, the majority of the heat addition came from the additional heat introduced by the power pack. Both stope environments were able to remove their heat successfully by dewatering their service water using a pump.

From Steps 6 and 7 of the method, *Objective 1.2: Compare and validate simulation results to a real-world stope environment* was achieved successfully by creating and validating a stope simulation model to within 5% of the real-world stope environment. Thus, *Objective 1: Simulate the heat load characteristics of a stope environment* was achieved in Steps 1–7 of the stope heat load method.

Step 8 successfully achieved *Objective 2.1: Determine effect of the heat addition/removal on the stope environment conditions* by adding the quantified heat load of Objective 1.1 into the validated stope simulation model of Objective 1.2. The resulting addition of heat in the micro-hydropower stope environment increased the stope reject wet-bulb temperature by 0.6 °C and the dry-bulb temperature by 2.1 °C over the conventional stope environment.

Finally, Step 9 achieved *Objective 2.2: Analysis of the environmental effect if multiple stopes are converted* by determining that the temperature increase in a converted micro-hydropowered stope should be taken into consideration as the temperature increase is compounded along the raise line with the third stope in series having a 1.8 ° C higher reject wet-bulb temperature. Thus, *Objective 2: Predict thermal changes when introducing micro-hydropower technologies* was achieved in Steps 8 and 9 of the stope heat load method.

3.4 Conclusion

By applying the developed stope heat load method on the case study mine, the micro-hydropowered stope environment was seen to increase the ambient temperatures in the stope compared with those of a conventional stope. This increase in temperature should be taken into consideration when implementing micro-hydropowered technologies as an increase in temperature will reduce the productivity of labourers and increase their risk of heat injuries relative to a conventionally powered stope environment.

CHAPTER 4 – CONCLUSION

4.1 Preamble

This chapter provides an overview of the previous chapters and highlights the main findings. The identified study objectives are discussed to illustrate how they were achieved.

4.2 Study summary

Most conventional underground mines in South Africa utilise compressed-air handheld rock drills. However, the ageing compressed-air reticulation networks are becoming increasingly inefficient due to their complexity and misuse. This leads to a reduction in the compressed-air pressure seen in stopes, which reduces the penetration rates of handheld rock drills and thus reduces production. As a result, alternative drilling technologies have become more prevalent in the industry.

These alternative technologies include hydropower, electro-hydraulic and electric handheld rock drills. All these alternative technologies negate the need for compressed air for drilling. However, these technologies move their respective power generation units (electric motors and pumps) into the stope environment (adding heat), whereas conventional compressed-air networks situate their compressed-air generation units outside the boundary of concern.

Excessive heat in the working environment can lead to heat injuries such as heat cramps, heat exhaustion and heatstroke, which can cause serious harm in extreme cases. Furthermore, the production efficiency of labourers is directly correlated to the temperature of the local environment as an increase in temperature will decrease the production efficiency of labourers.

A literature review was conducted to review the knowledge base on heat load effects of alternative drilling technologies in the stope environment. Studies focusing on the simulation of mining ventilation were investigated. This led to the identification of a gap in the literature whereby the heat load effect of alternative drilling technologies on the stope environment is largely undetermined. Of the three main alternative drilling technologies, micro-hydropower introduces the largest power requirement per drill into the stope environment and has the highest instantaneous water usage. Thus, this led to the development of the problem statement of this study, namely: “There exists a need to quantify the heat load of micro-hydropowered stope environments.”

To fulfil the gap identified by the problem statement, two study objectives were developed:

1. Simulate the heat load characteristics of a stope environment.
    1.1. Quantify heat added/removed from the environment.
    1.2. Compare and validate simulation results to a real-world stope environment.
2. Predict thermal changes when introducing micro-hydropower technologies.
    2.1. Determine effect of the heat addition/removal on the stope environment conditions.
    2.2. Analysis of the environmental effect if multiple stopes are converted.

In Chapter 2, a stope heat load method was developed from the learnings from Chapter 1. The method aimed to address each of the identified objectives by applying a general case study research methodology.

In Chapter 3, the developed stope heat load method was implemented on a case study platinum mine in South Africa where a conventional compressed-air stope environment was converted to a micro-hydropowered stope. The heat load over the conventional and micro-hydropowered stopes was evaluated and the nett heat load effect was determined and validated through simulation. The case study results are summarised in the following section.

4.3 Findings

A conventional pneumatic stope environment and converted micro-hydropowered stope were benchmarked according to the developed method. From this data, the heat load over the stope was analysed and it was found that the compressed-air drills removed 2.8 kW of heat from the localised environment (Objective 1.1). Thereafter, the heat load over the hydropower stope was analysed. The 55 kW hydropower power pack was seen to add 46.2 kW of heat to the service water in the stope. Of the 46.2 kW added to the stope, 6 kW of heat was liberated to the localised environment (Objective 1.1), and the remaining 40.2 kW was dewatered from the stope through good water controls.

A simulation model for the compressed-air stope environment was created with the determined heat load characteristics and the results were validated against a real-world stope environment (Objective 1.2). Thereafter, the heat load characteristics of the hydropowered stope environment was incorporated into the validated simulation. The hydropowered stope was shown to increase the reject wet-bulb temperature of the stope by 0.6 °C compared with the conventional pneumatic stope environment (Objective 2.1). The reject temperatures of stopes in series were also investigated, replicating a raise line.

The reject temperatures of the hydropowered stopes in series were higher than those of the compressed-air stopes. By the third stope in series, the hydropower stope exceeded the legal temperature limit. The reject wet-bulb temperature was 34.0 °C, which is 1.8 °C higher than that of the third compressed-air stope. This implies that the micro-hydropower raise line would be at a greater risk of heat injuries and that labourer efficiency would be reduced as a result of the higher temperatures. Depending on the micro-hydropower application, a raise line conversion can result in fewer active stopes than the compressed-air alternative due to the increased reject temperatures (objective 2.2).

Considering the objectives set out for this study, the heat load characteristics of a stope environment were simulated and the thermal changes when introducing micro-hydropower technologies were predicted. Thus, the objectives of this study were achieved successfully.

4.4 Shortcomings and recommendations

The following shortcomings in the study have been identified:

The ventilation airflow through the stope environment was non-uniform and made the temperature prediction difficult. In order to combat the real-world temperature distribution, multiple temperature loggers should be placed at fixed relative locations in the stope environment during drilling operations. The locations will have to move with the progression of the face and thus the relative locations will need to remain constant. From this, a temperature heat map of the stope can be created and replicated in the simulation model with a more intricate mesh-like CFD simulation approach. The ventilation air velocity should also be recorded multiple times in various locations to characterise the stope ventilation flow distribution better.

The recommendations for future work are summarised as follows:

Predict the thermal changes when introducing other alternative drilling technologies

The heat load effect on the stope environment can be quantified for other alternative drilling technologies such as electric and electro-hydraulic technologies.

Predict the thermal changes when service water is recirculated in micro-hydropower applications

Hydropowered drills can recirculate up to 70% of their service water, which reduces the dewatering volumes of the stope. The recirculated water is pumped back into the stope's water supply, which also reduces the instantaneous water demand the mine needs to supply. However, it is predicted that the recirculated water will increase the water temperature in the network, thus the heat load effect of the water recirculation on the stope environment should be quantified. This study could be expanded to the variation of service water temperatures and their effect on the stope's heat load. From this, a general heat prediction model could be built whereby the stope intake parameters are specified for an individual case study. The model will provide accurate predictions of the stope reject parameters; alternatively, the model could specify the required inlet parameters to meet a specified reject parameter.

Investigate the effect of dewatering controls on the stope's heat load

As seen in the case study environment, the dewatering controls implemented provided for sufficient removal of water. However, if the dewatering controls allowed for the wastewater to pool for longer periods, the water temperature will tend to that of the ambient rock temperature. This may increase the latent heat transfer in the stope and worsen the stopes ambient air conditions.

4.5 Concluding remarks

The results of this study will aid the underground mining industry in its decision-making when considering micro-hydropower technologies for their existing stope environments. This stope heat load method enables mines to determine the nett heat load effect on the stope environment when converting existing conventional stope environments to micro-hydropowered stope environments.

This method will allow the underground mining industry to plan accordingly when considering micro-hydropowered technologies and will hopefully prevent excessive heat in stope environments as a result of the conversion. Additional heat is added to the stope environment – if not managed correctly or accounted for, it may increase the temperature in the stope environment past legal limits or reduce the production efficiency of labourers, negating or outweighing any production benefits of the alternative drilling technology.

REFERENCE LIST

[1] S. Chistyakova, R. Latypov, and K. Youlton, “Multiple Merensky Reef of the Bushveld Complex, South Africa,” *Mineralogy and Petrology*, vol. 174, no. 3, Mar. 2019, doi: 10.1007/s00410-019-1562-x.

[2] R. G. Cawthorn and K. Boerst, “Origin of the pegmatitic pyroxenite in the Merensky Unit, Bushveld Complex, South Africa,” *Petrology*, vol. 47, no. 8, pp. 1509–1530, Aug. 2006, doi: 10.1093/petrology/egl017.

[3] O. Bamisaiye, P. Eriksson, J. van Rooy, H. Brynard, S. Yoya, A. Billay, V. Nxumalo and A.M. Adeola, “Subsurface geometry of the northwestern Bushveld Complex, South Africa [Géométrie tridimensionnelle de la partie nord-ouest du Complexe de Bushveld, Afrique du Sud],” *Canadian Journal of Tropical Geography [Revue Canadienne de Géographie Tropicale]*, vol. 3, pp. 2292–4108, May 2016.

[4] F. Egerton, “Presidential address: The mechanisation of UG2 mining in the Bushveld Complex,” *Journal of the South African Institute of Mining and Metallurgy*, vol. 104, pp. 439–450, Sep. 2004.

[5] R. J. Kendall and M. Gericke, “Mechanization in stoping narrow tabular orebodies,” *Journal of the South African Institute of Mining and Metallurgy*, vol. 100, pp. 135–143, Mar. 2000.

[6] K. A. Moxham, “A hard rock narrow reef mining machine: ARM 1100,” *Journal of the South African Institute of Mining and Metallurgy*, pp. 207–214, Oct. 2004.

[7] Nong Setshaba, “Review of successes and failures of mechanisation trials on platinum mines of the Bushveld Complex,” MSc Eng dissertation, University of the Witwatersrand, Johannesburg, 2010.

[8] F. Fourie, P. Valicek, G. Krafft, and J. Sevenoaks, “Narrow-reef mechanized mining layout at Anglo American Platinum,” *Journal of the South African Institute of Mining and Metallurgy*, vol. 117, no. 3, pp. 263–274, Mar. 2017, doi: 10.17159/2411-9717/2017/v117n3a8.

[9] P. G. Andrews, R. J. Butcher, and J. Ekkerd, “The geotechnical evolution of deep-level mechanized destress mining at South Deep mine,” *Journal of the South African Institute of Mining and Metallurgy*, vol. 120, 2020, doi: 10.17159/2411-9717/854/2020.

[10] A. J. Naldrett, A. Wilson, J. Kinnaird, and G. Chunnett, “PGE tenor and metal ratios within and below the Merensky Reef, Bushveld Complex: Implications for its genesis,” *Petrology*, vol. 50, no. 4, pp. 625–659, May 2009, doi: 10.1093/petrology/egp015.

[11] S. Xu, R. Liang, F. T. Suorineni, and Y. Li, “Evaluation of the use of sublevel open stoping in the mining of moderately dipping medium-thick orebodies,” *International Journal of Mining Science and Technology*, vol. 31, no. 2, pp. 333–346, Mar. 2021, doi: 10.1016/j.ijmst.2020.12.002.

[12] P. Fraser, “Saving energy by replacing compressed air with localized hydropower systems: A ‘half level’ model approach,” in *Proceedings of the International Platinum Conference Platinum in Transformation*, The Southern African Institute of Mining and Metallurgy, 2008, pp. 285–292.

[13] C. J. J. Van Zyl, “Practical approach to analyse mine pneumatic drilling performance,” MEng dissertation, North-West University, Potchefstroom, 2019.

[14] J. I. Phillips, P. S. Heyns, and G. Nelson, “Rock drills used in South African mines: A comparative study of noise and vibration levels,” *The Annals of Occupational Hygiene*, vol. 51, no. 3, pp. 305–310, Apr. 2007, doi: 10.1093/annhyg/mel082.

[15] Boart Longyear, “S250 rock drill: Rock drill & blast equipment and technical overview,” Salt Lake City, UT, 2012. Accessed: Sep. 9, 2022. [Online]. Available: https://www.distribucionespako.com/galeria_inf/i83_397.pdf.

[16] K. Naidoo and M. F. Handley, “Basic principles for stable gullies in the gold and platinum mines of South Africa,” *Journal of the South African Institute of Mining and Metallurgy*, vol. 102, no. 4, pp. 189–198, May 2002.

[17] I. M. Klotz and R. M. Rosenberg, “Application of the first law to gases,” in *Handbook: Chemical Thermodynamics Basic Concepts and Methods*, 7th ed. Hoboken, NJ: Wiley & Sons, 2008, pp. 90–94.

[18] A. Van Jaarsveld, S. Ebben, and AngloGold Ashanti, “Development and implementation of an electrically powered stope rock drill for Tau Tona mine,” in *Proceedings of the Narrow Vein and Reef Conference*, Sun City, South Africa: SAIMM, 2008.

[19] J. Wills, “Hydropower and stope drilling systems: An energy-saving perspective,” in *Proceedings of the Narrow Vein and Reef Conference* , Sun City, South Africa: SAIMM, 2008.

[20] J. H. Marais, “An integrated approach to optimise energy consumption of mine compressed air systems,” PhD dissertation, North-West University, Potchefstroom, 2012.

[21] C. Cilliers, “Benchmarking electricity use of deep-level mines,” PhD dissertation, North-West University, Potchefstroom, 2016.

[22] P. Fraser, “The energy and water required to drill a hole,” in *Proceedings of the 4th International Platinum Conference. Platinum in Transition ‘Boom or Bust’,* Sun City, South Africa: SAIMM, Oct. 2010, pp. 211–222.

[23] Atlas Copco, “Pneumatic rock drills: Rock drill sales,” GA, USA, Sep. 2015. Accessed: Jun. 4, 2022. [Online]. Available: https://airstart.com.au/pdf/AtlasCopco_Pneumatic-Rock-Drills_Catalogue_ALL.pdf.

[24] P. D. Fraser, “Hydropower: A mature, game-changing technology,” in *Proceedings of the 6th International Platinum Conference. Platinum-Metal for the Future*, Johannesburg, South Africa: SAIMM, Oct. 2014, pp. 39–48.

[25] Morris Lubricants, “Safety data sheet: Aria EP 220 rock drill oil,” Shrewsbury, Nov. 2015. Accessed: Jul. 2, 2023. [Online]. Available: https://www.morrislubricants.co.uk/products/236_5fabf2c229223.pdf.

[26] P. Nowak, K. Kucharska, and M. Kamiński, “Ecological and health effects of lubricant oils emitted into the environment,” *International Journal of Environmental Research and Public Health*, vol. 16, no. 16, Aug. 2019, doi: 10.3390/ijerph16163002.

[27] S. Z. Mafokwane and D. V. V Kallon, “Design of electro-hydraulic circuits of tri-adjustable automated heavy-duty industrial handling system,” in *Proceedings of the African International Conference on Industrial Engineering and Operations Management*, Harare, Zimbabwe, Dec. 2020, pp. 357–367.

[28] Epiroc, “HRD100 Hydraulic rock drill,” Stockholm, Sweden, Sep. 2020. Accessed: May. 27, 2022. [Online]. Available: https://www.epiroc.com/content/dam/epiroc/rock-drilling-tools/documents/Epiroc%20HRD100%20Hydraulic%20Rock%20Drill%20brochure.pdf.

[29] F. Fourie, P. Valicek, G. Krafft, and D. Baird, “A new electro hydraulic hand held rock drill tested by Anglo American NMT,” Anglo American, South Africa, 2017.

[30] HILTI, “TE MD20 LS T: Operating instructions,” Schaan, Liechtenstein, Apr. 2017. Accessed: May. 28, 2022. [Online]. Available: https://manualmachine.com/hilti/temd20lst/2580521-user-manual/.

[31] F. M. Menschik, “Analysis of performance and wear of electrical rock hammer drills,” PhD dissertation, Technischen Universität München, Munich, 2015.

[32] P. J. Petit, “Electric rock drilling system for in-stope mining in platinum operations,” in *Proceedings of the International Platinum Conference “Platinum Surges Ahead,”* Sun City, South Africa, 2006, pp. 209–216.

[33] G. Seetal, “Evaluating water supply control at a centralised hydro-powered mine,” MEng dissertation, North-West University, Potchefstroom, 2021.

[34] P. J. Petit and P. D. Fraser, “What is the best energy-delivery system for hand-held stope drilling and associated equipment in narrow-reef hard rock mines?,” *Journal of Southern African Institute of Mining and Metallurgy*, vol. 113, no. March, pp. 243–249, 2013.

[35] P. D. Fraser, “Hydropower technology can assist in meeting the safety and health ‘2013 milestones’ and save energy: A case for ‘localized’ hydropower systems in general and hydropowered stope drill rigs in particular,” in *Proceedings of the 4th International Platinum Conference, Platinum in Transition ‘Boom or Bust’,* Sun City, South Africa, 2010.

[36] T. Maurya, K. Karena, H. Vardhan, M. Aruna, and M. G. Raj, “Potential sources of heat in underground mines: A review,” *Procedia Earth and Planetary Science*, vol. 11, pp. 463–468, Jan. 2015, doi: 10.1016/J.PROEPS.2015.06.046.

[37] X. Nie, X. Wei, X. Li, and C. Lu, “Heat treatment and ventilation optimization in a deep mine,” *Advances in Civil Engineering*, 2018, Accessed: Nov. 28, 2021. [Online]. Available: doi: 10.1155/2018/1529490.

[38] D. W. Stanton, J. Kielblock, and J. J. Schoeman, *Handbook on Mine Occupational Hygiene Measurements*. Johannesburg: MHSC, 2007.

[39] Z.-g Su, Z.-a Jiang, and Z.-g. Sun, “Study on the heat hazard of deep exploitation in high-temperature mines and its evaluation index,” *Procedia Earth and Planetary Science*, vol. 1, no. 1, pp. 414–419, Sep. 2009, doi: 10.1016/J.PROEPS.2009.09.066.

[40] S. Roy, D. P. Mishra, R. M. Bhattacharjee, and H. Agrawal, “Heat stress in underground mines and its control measures: A systematic literature review and retrospective analysis,” *Mining, Metallurgy & Exploration*, vol. 39, no. 2, pp. 357–383, 2022, doi: 10.1007/s42461-021-00532-6.

[41] Department of Mineral Resources, *Mine Health and Safety Act, 1996 (Act No. 29 of 1996),* 14th ed. LexisNexis, 2018.

[42] D. Clement, “A comparison between hydraulic and pneumatic rockdrills,” *Journal of the South African Institute of Mining and Metallurgy*, p. 218, Mar. 1975.

[43] F. Wei, Z. Fangping, and L. Huiqing, “The use of 3D simulation system in mine ventilation management,” *Procedia Engineering*, vol. 26, pp. 1370–1379, 2011, doi: 10.1016/j.proeng.2011.11.2313.

[44] E. De Souza, “Optimization of complex mine ventilation systems with computer network modelling,” *IFAC Proceedings Volumes*, vol. 40, no. 11, pp. 323–329, 2007, doi: 10.3182/20070821-3-CA-2919.00049.

[45] R. Fair, “Optimisation of mine secondary fan systems,” MEng dissertation, North-West University, Potchefstroom, 2019.

[46] D. Nell, “Practical determination of heat loads for existing deep level gold mines,” PhD dissertation, North-West University, Potchefstroom, 2020.

[47] A. J. H. Nel, J. C. Vosloo, and M. J. Mathews, “Evaluating complex mine ventilation operational changes through simulations,” *Energy in Southern Africa*, vol. 29, no. 3, pp. 22–32, Aug. 2018, doi: 10.17159/2413-3051/2018/v29i3a4445.

[48] E. S. Manon, *Transmission Pipeline Calculations and Simulations Manual*. Houston, TX: Elsevier, 2015.

[49] F. H. Von Glehn, R. Hemp, and R. C. Funnell, “Numerical modelling of heat flow in mines,” *South African Journal of Science*, vol. 98, no. 9, pp. 485–490, Sep. 2002.

[50] V. Chauhan, “Optimization of parameters to improve ventilation in underground mine working using CFD,” MEng dissertation, National Institute of Technology, Rourkela, 2014.

[51] A. J. H. Nel, “Mine ventilation characterisation through simulations,” PhD dissertation , North-West University, Potchefstroom, 2018.

[52] S. Crowe, K. Cresswell, A. Robertson, G. Huby, A. Avery, and A. Sheikh, “The case study approach,” *BMC Medical Research Methodology*, vol. 11, p. 100, Jun. 2011, doi: 10.1186/1471-2288-11-100.

[53] W. Tellis, “Application of a case study methodology,” *The Qualitative Report*, vol. 3, no. 3, pp. 1–19, Sep. 1997, doi: 10.46743/2160-3715/1997.2015.

[54] A. Priya, “Case study methodology of qualitative research: Key attributes and navigating the conundrums in its application,” *Sociological Bulletin*, vol. 70, no. 1, pp. 94–110, Nov. 2021, doi: 10.1177/0038022920970318.

[55] S. Teegavarapu, J. Summers, and G. Mocko, “Case study method for design research: a justification,” in *Proceedings of the ASME Design Engineering Technical Conference*, New York, NY, USA, Aug. 2008, pp. 1–9. doi: 10.1115/DETC2008-49980.

[56] C. Quintão, P. Andrade, and F. Almeida, “How to improve the validity and reliability of a case study approach?,” *Interdisciplinary Studies in Education*, vol. 9, no. 2, pp. 273–284, Aug. 2020, doi: 10.32674/JISE.V9I2.2026.

[57] A. J. H. Nel, J. C. Vosloo, and M. J. Mathews, “Supplementary file: Evaluating complex mine ventilation operational changes through simulations,” *Journal of Energy in Southern Africa*, vol. 29, no. 3, 2018.

[58] M. J. McPherson, *Subsurface Ventilation and Environmental Engineering*, 2nd ed. Berlin, Germany: Springer Science & Business Media, 2012.

[59] J. Watkins, “Trade-off between simulation accuracy and complexity for mine compressed air systems,” MEng dissertation , North-West University, Potchefstroom, 2019.

[60] R. D. Clarke, “A framework for life of mine ventilation planning with a case study of the Diavik diamond mine,” MEng dissertation, Queen’s University, Kingston, 2017.

[61] T. Naldrett, J. Kinnaird, A. Wilson, and G. Chunnett, “Concentration of PGE in the Earth’s crust with special reference to the Bushveld Complex,” *Earth Science Frontiers*, vol. 15, pp. 264–297, Sep. 2008, doi: 10.1016/S1872-5791(09)60006-3.